Published in final edited form as:
Neurobiol Dis. 2009 August ; 35(2): 219–233. doi:10.1016/j.nbd.2009.05.001.

DENDRITIC SPINE PATHOLOGIES IN HIPPOCAMPAL PYRAMIDAL NEURONS FROM RETT SYNDROME BRAIN AND AFTER EXPRESSION OF RETT-ASSOCIATED *MECP2* MUTATIONS

Christopher A. Chapleau[1], **Gaston D. Calfa**[1], **Meredith C. Lane**[1], **Asher J. Albertson**[1], **Jennifer L. Larimore**[1], **Shinichi Kudo**[2], **Dawna L. Armstrong**[3], **Alan K. Percy**[4], and **Lucas Pozzo-Miller**[1]

[1]Department of Neurobiology, Evelyn McKnight Brain Institute, Civitan International Research Center, The University of Alabama at Birmingham (UAB), Birmingham, AL 35294-2182, USA

[2]Hokkaido Institute of Public Health, Kita-19, Nishi-12, Kita-ku, Sapporo 060-0819, Japan

[3]Department of Pathology, Baylor College of Medicine, Houston, Texas 77030

[4]Department of Pediatrics, UAB, Birmingham, AL 35294-2182, USA.

Abstract

Rett syndrome (RTT) is an X chromosome-linked neurodevelopmental disorder associated with the characteristic neuropathology of dendritic spines common in diseases presenting with mental retardation (MR). Here, we present the first quantitative analyses of dendritic spine density in postmortem brain tissue from female RTT individuals, which revealed that hippocampal CA1 pyramidal neurons have lower spine density than age-matched non-MR female control individuals. The majority of RTT individuals carry mutations in *MECP2*, the gene coding for a methylated DNA-binding transcriptional regulator. While altered synaptic transmission and plasticity has been demonstrated in *Mecp2*-deficient mouse models of RTT, observations regarding dendritic spine density and morphology have produced varied results. We investigated the consequences of MeCP2 dysfunction on dendritic spine structure by overexpressing (~twofold) MeCP2-GFP constructs encoding either the wildtype (WT) protein, or missense mutations commonly found in RTT individuals. Pyramidal neurons within hippocampal slice cultures transfected with either WT or mutant *MECP2* (either R106W or T158M) showed a significant reduction in total spine density after 48hrs of expression. Interestingly, spine density in neurons expressing WT *MECP2* for 96hrs was comparable to that in control neurons, while neurons expressing mutant *MECP2* continued to have lower spines density than controls after 96hrs of expression. Knockdown of endogenous *Mecp2* with a specific small hairpin interference RNA (shRNA) also reduced dendritic spine density, but only after 96hrs of expression. On the other hand, the consequences of manipulating MeCP2 levels for dendritic complexity in CA3 pyramidal neurons were only minor. Together, these results demonstrate reduced dendritic spine density in hippocampal pyramidal neurons from RTT patients, a distinct

Contact information: Lucas Pozzo-Miller, Ph.D., Department of Neurobiology, SHEL-1002, The University of Alabama at Birmingham, 1825 University Blvd. Birmingham, AL 35294-2182, USA, **Phone:** 205.975.4659, **Fax:** 205.934.6571, **E-mail:** lucaspm@uab.edu.

dendritic phenotype also found in neurons expressing RTT-associated *MECP2* mutations or after shRNA-mediated endogenous *Mecp2* knockdown, suggesting that this phenotype represent a cell-autonomous consequence of MeCP2 dysfunction.

Keywords

MeCP2; Rett syndrome; dendrite; dendritic spine; pyramidal neuron; hippocampus; DiOlistics; human postmortem brain

INTRODUCTION

Deficits in dendritic architecture are common in disorders associated with mental retardation (MR), ranging from environmental (e.g. fetal alcohol syndrome) to autosomal (e.g. Down syndrome) and X chromosome-linked forms of MR (e.g. Fragile-X, Rett syndrome; reviewed by Fiala *et al*., 2002; Kaufmann and Moser, 2000). A series of groundbreaking studies published in the 1970's established the precedent of abnormalities in dendritic organization in cortical neurons from humans with MR (Huttenlocher, 1970; Huttenlocher, 1974; Marin-Padilla, 1972; Marin-Padilla, 1976). These series of observations consistently described reductions in the density of dendritic spines, the postsynaptic compartment of excitatory synapses (reviewed by Peters *et al*., 1991). In addition, a prevalence of long and tortuous spines, thought to represent immature synapses, were also commonly observed in MR and combined, these dendritic spine anomalies were referred to as "spine dysgenesis" (Purpura, 1974). Since dendritic development is a process where the formation and maturation of spines are the result of interactions between intrinsic genetic factors and external environment, the study of spine development and maintenance in MR has significant clinical relevance.

Rett syndrome (RTT) is an X chromosome-linked mental retardation that results from sporadic mutations in the gene coding for the methylated DNA-binding transcription factor MeCP2 (Amir *et al*., 1999; reviewed by Percy, 2001). RTT affects approximately 1:10,000 females worldwide, and prominent symptoms include deceleration of body and head growth rate, hand stereotypies and regression in motor and speech capabilities, irregularities in motor activity and breathing patterns, in addition to cognitive impairments characteristic of an autism-spectrum disorder (reviewed by Percy and Lane, 2005). Although RTT occurs predominantly in females, mutations of *MECP2* have also been identified in males, where the phenotypes range from severe encephalopathy, to classic RTT, to nonspecific MR (Couvert *et al*., 2001; Kankirawatana *et al*., 2006; Masuyama *et al*., 2005; Moog *et al*., 2003). While mutations of *MECP2* have been associated with RTT, duplications in the chromosomal region where *MECP2* is located were shown to be related to neurological disorders associated with MR, suggesting that *MECP2* is a critical dosage-sensitive gene (del Gaudio *et al*., 2006; Smyk *et al*., 2008).

Morphological studies in postmortem brain samples from RTT individuals described a characteristic neuropathology, which included decreased neuronal size and increased neuronal density in the cerebral cortex, hypothalamus and the hippocampal formation (Bauman *et al*., 1995a; Bauman *et al*., 1995b); decreased dendritic growth in pyramidal neurons of the subiculum and frontal and motor cortices (Armstrong *et al*., 1995); as well as the characteristic MR-associated spine dysgenesis, observed in pyramidal neurons of the motor cortex with regions of dendrites devoid of spines (Belichenko *et al*., 1994). The reduction in dendritic area together with the marked decrease in dendritic spine density strongly suggests that impaired synaptic transmission is a likely pathogenic consequence of *MECP2* mutations causing RTT. Indeed, the increase in neuronal expression of *MECP2/Mecp2* during early brain development suggests the importance of this protein in synapse formation and maintenance (Akbarian *et*

al., 2001; Cassel *et al*., 2004; Jung *et al*., 2003; Kaufmann *et al*., 2005; Mullaney *et al*., 2004; Shahbazian *et al*., 2002b). While hippocampal and cortical synaptic dysfunction in *Mecp2*-based mouse models of RTT has been extensively studied, observations regarding neuronal, dendritic and synaptic pathologies have produced varied results (Asaka *et al*., 2006; Chao *et al*., 2007; Dani *et al*., 2005; Fukuda *et al*., 2005; Gemelli *et al*., 2006; Jugloff *et al*., 2005; Kishi and Macklis, 2004; Moretti *et al*., 2006; Nelson *et al*., 2006; Smrt *et al*., 2007; Zhou *et al*., 2006). Here, we present the first quantitative analyses of dendritic spine density in postmortem brain tissue from RTT individuals. To identify the consequences of cell-autonomous MeCP2 dysfunction on the morphology of dendrites and dendritic spines in hippocampal pyramidal neurons, we transfected organotypic slice cultures with either wildtype or RTT-associated *MECP2* mutations.

MATERIAL AND METHODS

HUMAN POSTMORTEM BRAIN

All procedures on human postmortem brain samples followed national and international ethics guidelines, and were reviewed and approved by the Institutional Review Board (IRB) at The University of Alabama at Birmingham (UAB). Brain sections containing the hippocampal formation were obtained from individuals diagnosed with RTT, and unaffected (non-MR) individuals served as controls. Post-mortem human tissue was obtained from the Department of Pathology, Baylor College of Medicine, the NICHD Brain and Tissue Bank for Developmental Disorders at the University of Maryland, Baltimore, MD, and from the Harvard Brain Bank. Table 1 presents all the available information on the individuals whose brains were used in this study. Unfortunately, information about specific *MECP2* mutations in Rett syndrome samples is not available from the brain banks.

DIOLISTICS OF HUMAN POSTMORTEM HIPPOCAMPAL SLICES

Fixed human postmortem samples (received in 10% formalin) were first extensively washed in phosphate buffer saline (PBS), and then sectioned at 200μm thickness with a vibratome to isolate the hippocampus (Supplemental Figure 1A). Tissue slices were stained with the lipophilic dye, 1,1′-dioctadecyl-3,3,3′,3′-tetramethylindocarbocyanine perchlorate (DiI, InVitrogen; Carlsbad, CA) by particle-mediated labeling ("DiOlistics") (Gan *et al*., 2000). DiI was diluted in dimethyl chloride (methylene chloride, Sigma; St. Louis, MO). Twenty mg of 1.1μm tungsten particles (Bio-Rad; Hercules, CA) were placed on top of a pre-cleaned glass slide and spread out evenly with two pre-cleaned razor blades. The DiI solution was added onto the tungsten particles and allowed to completely evaporate. To prevent clumping of the DiI/tungsten mixture, razor blades were used to break apart and separate the mixture. Additionally, polyvinlypirrollidone (PVP made in fresh in 100% ethanol, Bio-Rad) was added to the DiI/tungsten mixture to further prevent particle clumping and improve their coating to the Tefzel tubing. The DiI-coated tungsten particles were then added to a glass tube with 3mL of water and sonicated for 2hrs. After sonication, the solution was vortexed and then aspirated and coated onto Tefzel tubing for 3hrs. After 3hrs, the solution was removed and the tubing was allowed to dry for 2hrs. DiI-coated tungsten bullets were shot 2–4 times onto individual human hippocampal slices with a custom-modified hand-held gene gun (Helios, Bio-Rad) using 125psi He pressure through a 40μm-pore size filter (Alonso *et al*., 2004). After labeling with DiI bullets, slices were rinsed and stored in PBS for 24–36hrs at room temperature in the dark to allow diffusion of DiI. Then, slices were post-fixed with 4% paraformaldehyde and stored at 4°C overnight. Slices were finally washed with PBS and mounted on glass slides with Vectashield (Vector Laboratories; Burlingame, CA). Supplemental Figure 1B shows a bright-field example of tungsten bullets within a fixed human hippocampal slice, and the resulting DiI fluorescence.

ORGANOTYPIC SLICE CULTURES

All procedures on experimental animals followed national and international ethical guidelines, and were reviewed and approved by the IACUC at UAB on an annual basis. Hippocampal slice cultures were prepared from postnatal-day 7 to 10 (P7-P10) Sprague-Dawley rats and maintained *in vitro as* previously described (Stoppini *et al*., 1991). Briefly, rats were quickly decapitated and their brains aseptically dissected and immersed in ice-cold dissecting solution, consisting of Hanks' Balanced Salt Solution (HBSS), supplemented with glucose (36mM) and antibiotics/antimycotics (1:100; penicillin/streptomycin/amphotericin-B). Hippocampi were then dissected and transversely sectioned into ~500μm slices using a custom-made tissue slicer (Katz, 1987) strung with 20μm-thick tungsten wire (California Fine Wire Company; Grover Beach, CA). Slices were incubated at 4oC for ~30min, and then plated on tissue culture inserts (0.4μm pore size, Millicell-CM, Millipore Corporation; Billerica, MA). Culture media contained minimum essential media (MEM; 50%), HBSS (25%), heat-inactivated equine serum (20%), L-glutamine (1mM), and D-glucose (36mM). Slice cultures were maintained in incubators at 36oC, 5% CO_2, 98% relative humidity (Thermo-Forma, Waltham, MA). All tissue culture reagents were obtained from InVitrogen (Carlsbad, CA), except for glucose, which was obtained from Sigma (St. Louis, MO).

PARTICLE-MEDIATED GENE TRANSFER

Expression cDNA plasmids encoding small hairpin RNA (shRNA) interfering sequences were obtained from Origene (Rockville, MD). The expression plasmids encoding shRNA sequences are under the control of the human U6 promoter. shRNA interfering sequences consist of a 29-base pair target gene-specific sequence, a 7-base pair loop, followed by a 29-base pair reverse complementary sequence. The *MECP2*-specific shRNA sequence AATGAGACAGCAGTCTTATGCTTCCAGAA (sequence #2), reduced MeCP2 protein levels by 65%, estimated by quantitative Western blot analyses of PC12 cells co-transfected with human wt *MECP2* and shRNA plasmids (Supplemental Figure 2; Larimore *et al*., 2009). Consistently, MeCP2 expression levels were 55% lower in hippocampal neurons transfected with the same shRNA plasmid (sequence #2) than in untransfected neighboring neurons, as estimated by quantitative MeCP2 immunofluorescence (Supplemental Figure 2; Larimore *et al*., 2009). Another shRNA sequence, TCAATAACAGCCGCTCCAGAGTCAGTAGT, which did not affect MeCP2 expression, was used as a control for shRNA off-target effects. To overexpress MeCP2, expression cDNA plasmids encoding human WT *MECP2* were used as previously described (Kudo, 1998; Kudo *et al*., 2001; Kudo *et al*., 2003). Expression plasmids encoding *MECP2* mutations commonly identified in RTT individuals were constructed by site directed mutagenesis using PCR, where WT *MECP2* was used as a template (Kudo *et al*., 2001). MeCP2 was tagged with an enhanced green fluorescent protein (eGFP) that was used to allow identification of transfected cells. The MeCP2-eGFP construct was cloned into a cytomegalovirus (CMV) promoter expression vector. These expression vectors produced a twofold increase in MeCP2 protein expression compared to untransfected cultured neurons, as measured by quantitative MeCP2 immunofluorescence (Supplemental Figure 2; Larimore *et al*., 2009).

The above plasmid cDNAs were precipitated onto 50mg of 1.6μm-diameter colloidal Au at a ratio of 62.5μg of enhanced yellow fluorescent protein (eYFP; Clontech; Mountain View, CA) to 112.5μg of MeCP2-GFP (wildtype or mutant *MECP2*) and then coated onto Tefzel tubing. A similar protocol was used to coat Au bullets with shRNA interfering sequence plasmids to knockdown the expression of endogenous *Mecp2*. The pEYFP-C1 plasmid was under control of the human CMV promoter (Clontech). After 6–8 days *in vitro* (div), slice cultures were bombarded with Au particles accelerated by ~100psi He from a distance of 2cm using a hand-held gene gun (Helios, Bio-Rad) with a modified nozzle, as previously described (Alonso *et al*., 2004). The success rate of co-transfection of the same neuron with two cDNA plasmids

using the gene-gun has been demonstrated to be >90% (Boda *et al*., 2004; Moore *et al*., 2007), reducing the likelihood of analyzing eYFP-positive, MeCP2-negative neurons. After 48hrs or 96hrs post-transfection, hippocampal slice cultures were fixed by immersion in 4% paraformaldehyde in 100mM phosphate buffer (overnight at 4°C), and washed in PBS. Filter membranes around each slice were trimmed, and each slice was individually mounted on glass slides and cover slipped using Vectashield (Vector Laboratories; Burlingame, CA).

LASER-SCANNING CONFOCAL MICROSCOPY

High-resolution images of spiny dendrites in the CA1 region of the human hippocampus showing adequate DiI labeling were acquired with a Fluoview FV-300 laser-scanning confocal microscope (Olympus; Center Valley, PA) using an oil immersion 100X (NA 1.4) objective lens (PlanApo, Olympus), or with a Leica TCS NT SP2 confocal using an oil immersion 100X (NA 1.4) objective lens (Leica; Exton, PA). DiI was excited using a Kr laser (647nm), and detected using standard Texas red filters. Series of optical sections in the z-axis were acquired with 0.1–0.2μm intervals through individual apical dendritic branches.

Pyramidal neurons located in the CA1 and CA3 regions of hippocampal slice cultures displaying eYFP fluorescence throughout the entire dendritic tree and lacking signs of degeneration (e.g. dendritic blebbing) were selected for confocal imaging. High-resolution images of secondary and tertiary branches of apical dendrites were acquired with a Fluoview FV-300 laser-scanning confocal microscope (Olympus) using an oil immersion 100X (NA 1.4) objective lens (PlanApo). eYFP was excited using an Ar laser (488nm), and detected using standard FITC filters. Series of optical sections in the z-axis were acquired at 0.1μm intervals through individual apical dendritic branches.

QUANTITATIVE ANALYSIS OF DENDRITIC SPINE DENSITY AND MORPHOLOGY

Dendritic spines were identified as small protrusions that extended ≤ 3μm from the parent dendrite, and counted in maximum-intensity projections of the z-stacks using ImageJ software (National Institutes of Health). Care was taken to ensure that each spine was counted only once by following its projection course through the stack of z-sections. Spines were counted only if they appeared continuous with the parent dendrite. Spine density was calculated by quantifying the number of spines per dendritic segment, and normalized to 10μm of dendrite length. In addition, the categorization of different morphological spine types was performed as described (Tyler and Pozzo-Miller, 2003). Spine types were grouped as mature-shaped spines, which included type-I (stubby) and type-II (mushroom) shaped spines, or immature-shaped thin (type-III) spines, following published criteria (Boda *et al*., 2004). For the purposes of this study, we pooled dendritic spine densities from CA1 and CA3 pyramidal neurons because the types of spines in secondary and tertiary apical dendrites of CA1 and CA3 neurons (and the excitatory synapses on them) are structurally and functionally comparable: apical secondary and tertiary dendrites in CA3 and CA1 *stratum radiatum* receive afferent axons from CA3 pyramidal neurons, i.e. they are contacted by the same type of presynaptic neuron (reviewed in Spruston and McBain, 2007). Statistical comparisons supported this approach: spine density was not significantly different between CA1 and CA3 neurons in any of the experimental groups ($p>0.05$). Detailed information about quantitative analyses is presented in Table 2.

QUANTITATIVE ANALYSIS OF DENDRITIC MORPHOLOGY

Low-resolution images of entire CA3 pyramidal neurons were acquired with a Fluoview FV-300 laser-scanning confocal microscope (Olympus) using an oil immersion 20X (NA 0.5) objective lens (PlanApo). Series of optical sections in the z-axis were acquired at 0.5μm intervals. Dendritic complexity of CA3 pyramidal neurons was measured by a three-dimensional version of the classical Sholl analysis (Sholl, 1953) using the z-stacks of confocal optical sections with Neurolucida software (MicroBrigthField; Colchester, VT). To measure

dendritic complexity of traced apical dendrites, series of concentric three-dimensional spheres starting at the soma and spaced at 20μm intervals were used to measure the number of dendritic intersections as a function of the distance away from the soma (20–500μm), as described (Alonso *et al*., 2004).

STATISTICAL ANALYSES

All data were analyzed with two-tailed unpaired Student's t tests, two-way ANOVA (transfection condition x distance from the soma) followed by Bonferroni post-hoc test, or unweighted and weighted least square regression analyses using Prism (GraphPad; San Diego, CA); $p < 0.05$ was considered significant. All data are presented as mean±standard deviation of the mean (SD). Compromise Power Analyses were performed to determine the statistical power given the number of observations, sample means and standard deviations, using G*Power (Erdfelder *et al*., 1996). These power analyses yielded values of statistical Power (1-β; where β is the Type-II error) larger than 0.90 (i.e. 90% confidence of accepting the null hypothesis when is true).

Results

HIPPOCAMPAL CA1 PYRAMIDAL NEURONS FROM RTT INDIVIDUALS HAVE LOWER DENDRITIC SPINE DENSITY THAN THOSE FROM NON-MR INDIVIDUALS

The only prior study on the features of dendritic spines in RTT individuals was performed on cortical samples and lacked quantitative statistical analyses (Belichenko *et al*., 1994). To perform quantitative analyses of spine density in pyramidal neurons from human hippocampus, postmortem tissue was obtained from female RTT individuals that were 1 to 42 years of age, and compared to age-matched unaffected non-MR female individuals (see Table for all available information from the human brain banks). Unfortunately, information about specific *MECP2* mutations in Rett syndrome samples was not available from the brain banks. Individual hippocampal slices (200μm-thick) were stained with the lipophilic fluorescent dye DiI by particle-mediated labeling ("DiOlistics"), and dendritic spines were imaged by laser-scanning confocal microscopy (Supplemental Figure 1, and Fig. 1A, B). Quantitative analyses revealed significantly lower dendritic spine density in secondary and tertiary apical dendrites of CA1 pyramidal neurons from RTT individuals compared to unaffected (non-MR) individuals (RTT 6.1±2.1 spines per 10μm of apical dendrite, mean±SD, n=10 individuals, *vs*. non-MR 9.2±1.9 spines/10μm, n=9 individuals; two-tailed Student's t-test p=0.0044; Fig. 1C). Both un-weighted and weighted least square regression analyses yielded a lack of significant correlation between age and spine density in controls and RTT neurons (Fig. 1D). These quantitative analyses demonstrate that hippocampal CA1 pyramidal neurons from RTT individuals have lower spine densities than neurons from non-MR individuals.

OVEREXPRESSION OF RTT-ASSOCIATED *MECP2* MUTATIONS CAUSED A PERSISTENT REDUCTION IN DENDRITIC SPINE DENSITY IN HIPPOCAMPAL PYRAMIDAL NEURONS

The analysis of dendritic spine densities in human brains representing a static cell population, serves as a direct comparison with that of dendritic spine densities in dynamic slice cultures derived from rat, in each instance involving hippocampal neuron populations. Since RTT results from mutations in *MECP2* (Amir *et al*., 1999; reviewed by Percy, 2001), we investigated the morphological consequences of cell-autonomous expression of missense *MECP2* mutations commonly found in RTT individuals. Our cDNA expression plasmids use the CMV promoter, and the resulting protein levels are approximately twofold the endogenous MeCP2 levels, as estimated by quantitative MeCP2 immunocytochemistry (Supplemental Figure 2). We used single amino acid substitutions in the methyl-binding domain of MeCP2 (R106W or T158M), which alter its structure, methylated DNA binding and transcription repressive activity (Ghosh *et al*., 2008; Ho *et al*., 2008; Kudo *et al*., 2001; Kudo *et al*., 2003). We will

first describe the consequences of the overexpression of these RTT-associated *MECP2* mutations comparing dendritic spine density and morphology with eYFP-expressing control CA1 and CA3 pyramidal neurons, and in the following section present the results of the overexpression of wildtype human *MECP2*. It is important to note that the levels of endogenous *Mecp2* gene were not manipulated in these experiments. Since they receive comparable presynaptic input from CA3 pyramidal neurons (reviewed in Spruston and McBain, 2007), the densities of dendritic spines from secondary and tertiary apical dendrites of CA1 and CA3 neurons were pooled in the present studies. Statistical comparisons confirmed that spine densities were not significantly different between the studied CA1 and CA3 dendrites in any of the experimental groups, including after *MECP2/Mecp2* manipulations (two-tailed Student's t-test $p>0.05$).

Forty-eight hours after transfection of hippocampal slice cultures, secondary and tertiary apical dendritic branches of pyramidal neurons expressing the R106W mutation showed significantly lower dendritic spine density than eYFP-expressing control neurons (R106W = 4.9±1.7 spines/10μm, mean±SD, 11 cells from 10 slices, *vs*. eYFP = 9.3±3 spines/10μm, 25 cells from 15 slices; two-tailed Student's t-test $p<0.0001$). Expression of the T158M mutation also resulted in lower spine density in pyramidal neurons than in control neurons (4.9±1.5 spines/10μm, 25 cells from 22 slices, *vs*. eYFP controls; two-tailed Student's t-test $p < 0.0001$; Fig. 2A, B).

Considering the direct relationship between the morphology of dendritic spines and the maturation state and strength of excitatory synapses formed on them (reviewed by Kasai *et al*., 2003; Nimchinsky *et al*., 2002; Yuste *et al*., 2000), we classified dendritic spines into mature (consisting of stubby and mushroom spines) and thin spines, which are considered to represent immature spines (Boda *et al*., 2004; Tyler and Pozzo-Miller, 2003; reviewed by Harris, 1999). The overexpression of either the R106W mutation or the T158M mutation caused a significant decrease in the density of mature spines in pyramidal neurons [(R106W = 3.6±1.2 mature spines/10μm, *vs*. eYFP = 8.1±2.7 mature spines/10μm; two-tailed Student's t-test $p<0.001$); (T158M = 3.9±1.3 mature spines/10μm, *vs*. eYFP controls; two-tailed Student's t-test $p<0.001$)]. On the other hand, overexpression of either *MECP2* mutant did not affect the density of immature thin spines in pyramidal neurons [(R106W = 1.2±0.9 immature spines/10μm, *vs*. eYFP = 1.2±0.8 immature spines/10μm; two-tailed Student's t-test $p=0.9672$); (T158M = 0.98±0.7 immature spines/10μm, *vs*. eYFP controls; two-tailed Student's t-test $p=0.1813$)]. These results are illustrated in Figure 2C.

When hippocampal pyramidal neurons were allowed to overexpress the mutant forms of *MECP2* for an additional 2 days *in vitro* (div) – for a total of 4 div – their dendritic spine density continued to be lower than eYFP-expressing control neurons. After 4 div, pyramidal neurons expressing the T158M mutation had 5.6±2.7 spines/10μm (30 cells from 14 slices), compared to 8.4±3.1 spines/10μm in eYFP controls (31 cells from 23 slices; two-tailed Student's t-test $p=0.0004$). Similar results were observed in pyramidal neurons overexpressing the R106W mutant (R106W = 6.2±3.3 spines/10μm, 16 cells from 11 slices, *vs*. eYFP controls; two-tailed Student's t-test $p=0.0257$; Fig. 2D, E).

Similar to the total spine density, the loss of mature dendritic spines was also a persistent phenotype of mutant *MECP2*-expressing neurons. After 4 div, pyramidal neurons expressing the T158M mutation still showed a lower density of mature spines than eYFP control cells (T158M = 4.5±2.1 spines/10μm, *vs*. eYFP = 7.3±2.6 spines/10μm; two-tailed Student's t-test $p<0.0001$). The overexpression of mutation R106W also reduced mature spines in pyramidal neurons (R106W = 4.7±2.2 spines/10μm, *vs*. eYFP controls; two-tailed Student's t-test $p=0.0012$). On the other hand, expression of mutant *MECP2* forms did not change the density of thin spines after 4 div from transfection [(R106W = 1.6±1.3 immature spines/10μm, *vs*.

eYFP = 1.1±1 immature spines/10μm; two-tailed Student's t-test p=0.2129); (T158M = 1.1 ±0.8 immature spines/10μm, *vs*. eYFP controls; two-tailed Student's t-test p=0.986; Fig. 2F)].

THE OVEREXPRESSION OF WILDTYPE *MECP2* CAUSED A TRANSIENT REDUCTION OF SPINE DENSITY IN HIPPOCAMPAL PYRAMIDAL NEURONS

As a control for the overexpression of RTT-associated *MECP2* mutant forms, we next analyzed dendritic spine density and morphology in hippocampal pyramidal neurons after transfection of wildtype (WT) human *MECP2*, which results in a ~twofold increase in protein level (Supplemental Figure 2). Reminiscent of the effect of mutant *MECP2*, pyramidal neurons overexpressing WT *MECP2* for 2 days *in vitro* (div) showed lower spine densities than eYFP controls (WT *MECP2* = 6.6±2.1 spines/10μm, 18 cells from 16 slices, *vs*. eYFP = 9.3±3 spines/10μm, 25 cells from 15 slices; two-tailed Student's t-test p=0.0023; Fig. 3A, B). In addition, the density of mature spines was significantly lower in WT *MECP2*-expressing pyramidal neurons than in eYFP controls (WT *MECP2* = 5.3±1.5 spines/10μm, *vs*. eYFP = 8.1±2.7 spines/10μm; two-tailed Student's t-test p=0.0003). On the other hand, the density of immature thin spines was not affected in pyramidal neurons (WT *MECP2* = 1.4±1 spines/10μm, *vs*. eYFP = 1.3±0.8 spines/10μm; two-tailed Student's t-test p=0.5787; Fig. 3C).

In contrast to the persistent spine loss observed in neurons expressing RTT-associated *MECP2* mutations (Fig. 2E), the above effects of WT *MECP2* on dendritic spine density were transient. Four days after transfection, dendritic spine density in WT *MECP2*-expressing pyramidal neurons was comparable to that of control neurons expressing eYFP (WT *MECP2* = 7.8±2.5 spines/10μm, 23 cells from 10 slices, *vs*. eYFP = 8.4±3.1 spines/10μm, 31 cells from 23 slices; two-tailed Student's t-test p=0.4388; Fig. 3D, E). Furthermore, the density of mature spines was also comparable between controls and WT *MECP2*-expressing pyramidal neurons (WT *MECP2* = 6.8±2.2 spines/10μm, *vs*. eYFP = 7.3±2.6 spines/10μm; two-tailed Student's t-test p=0.457). As after 2 div, the density of immature thin spines was unaffected after 4 days of expression of WT *MECP2* (WT *MECP2* = 1.1±0.5 spines/10μm, *vs*. eYFP = 1.1±1 spines/10μm; two-tailed Student's t-test p=0.7534; Fig. 3F).

KNOCKDOWN OF ENDOGENOUS *MECP2* REDUCED THE DENSITY OF MATURE DENDRITIC SPINES IN HIPPOCAMPAL PYRAMIDAL NEURONS

Considering that *MECP2* mutations in RTT individuals are thought to be "loss-of-function" mutations (reviewed by Shahbazian *et al*., 2002a), and the observations that *Mecp2* deficient neurons form fewer excitatory synapses in culture, while *MECP2* overexpressing neurons form more excitatory synapses *in vitro* than cultured neurons from wildtype littermates (Chao *et al*., 2007), we next investigated the consequences of endogenous *Mecp2* knockdown. To this aim, pyramidal neurons in hippocampal slice cultures were transfected with plasmids encoding *MECP2*-specific shRNA interfering sequences. Hippocampal neurons transfected with these shRNA plasmids showed a significant reduction in MeCP2 expression levels compared to untransfected neighboring neurons, as estimated by quantitative MeCP2 immunofluorescence (Supplemental Figure 2). After 48hrs of *Mecp2* knockdown, dendritic spine density in pyramidal neurons was comparable to control neurons transfected with an inactive shRNA sequence (*MECP2* shRNA = 8.6±3.7 spines/10μm, 13 cells from 10 slices, *vs*. control shRNA = 9.6±2 spines/10μm, 12 cells from 10 slices; two-tailed Student's t-test p = 0.9925; Fig. 4A, B). Similarly, *Mecp2* shRNA knockdown did not affect the density of mature spines (*MECP2* shRNA = 7±2.8 spines/10μm, *vs*. control shRNA = 7.4±1.6 spines/10μm; two-tailed Student's t-test p=0.688) or immature thin spines in pyramidal neurons (*MECP2* shRNA = 1.6 ±1.3 spines/10μm, *vs*. control shRNA = 1.3±0.7 spines/10μm; two-tailed Student's t-test p=0.4629; Fig. 4C).

Since the effectiveness of shRNA-mediated knockdown depends on protein turnover, we examined dendritic spine density after 4 days of transfection with shRNA expression plasmids. Indeed, *Mecp2* shRNA knockdown significantly reduced dendritic spine density in pyramidal neurons (*MECP2* shRNA = 7±2.8 spines/10μm, 14 cells from 12 slices, *vs*. control shRNA = 9.1±2.7 spines/10μm, 21 cells from 11 slices; two-tailed Student's t-test p=0.0283; Fig. 4D, E). Similarly, the density of mature spines in *MECP2* shRNA-expressing pyramidal neurons was lower than that of control neurons (*MECP2* shRNA = 5.5±2.1 spines/10μm, *vs*. control shRNA = 8±2.2 spines/10μm; two-tailed Student's t-test p=0.0016). This loss of mature dendritic spines is specific, because the density of immature thin spines was unaffected in pyramidal neurons (*Mecp2* shRNA = 1.6±0.8 thin spines/10μm, *vs*. control shRNA = 1.1±0.6 thin spines/10μm; two-tailed Student's t-test p=0.0838; Fig. 4F).

OVEREXPRESSION OF WILDTYPE *MECP2* HAD A SMALL EFFECT ON DENDRITIC COMPLEXITY, WHILE KNOCKDOWN OF ENDOGENOUS *MECP2* TRANSIENTLY REDUCED DENDRITIC LENGTH AND BRANCHING IN CA3 PYRAMIDAL NEURONS

Another feature of neurodevelopmental disorders associated with mental retardation, such as RTT, is a reduction in the size and complexity of dendritic arbors (reviewed by Kaufmann and Moser, 2000). Pyramidal neurons from the cortex and subiculum of female RTT individuals and from a male individual with a *MECP2* deletion displayed reduced dendritic complexity compared to non-MR individuals (Armstrong *et al*., 1995; Schule *et al*., 2008). To determine the role of MeCP2 in the growth and branching of hippocampal neurons, we performed a three-dimensional Sholl analysis of dendritic complexity from z-stacks of confocal sections of CA3 pyramidal neurons overexpressing either wildtype or the RTT-associated T158M *MECP2* mutation, as well as after endogenous *Mecp2* knockdown with a specific shRNA.

After 2 days of transfection, T158M-expressing CA3 pyramidal neurons show a small, but statistically significant higher number of apical dendritic intersections with the Sholl spheres compared to eYFP controls (100μm from the soma: T158M 8±2.6 intersections, 7 cells from 6 slices, *vs*. eYFP 3.2±0.9, 13 cells from 7 slices; ANOVA, Bonferroni post-hoc test $p<0.05$; Fig. 5A, B). This increase is transient, since the number of dendritic intersections in T158M neurons was comparable to control levels after 4 days of expression (11 cells from 8 slices, *vs*. eYFP, 14 cells from 10 slices; ANOVA, Bonferroni post-hoc test $p>0.05$; Fig. 6A, B). The total dendritic length and number of dendritic branch points were not affected after 2 days of expression [(T158M = 3,441±1716μm, *vs*. eYFP = 3,193±864μm; ANOVA, Bonferroni post-hoc test p=0.6685) (T158M = 20.7±12.7 branch points, *vs*. eYFP = 23.6±7.5 branch points; ANOVA, Bonferroni post-hoc test p=0.5158)]. Similar results were observed after 4 days of transfection [(T158M = 2,870±1053μm, *vs*. eYFP = 3,627±1048μm; ANOVA, Bonferroni post-hoc test p=0.0746) (T158M = 19.55±11.7 branch points, vs. eYFP = 23.67±8.6 branch points; ANOVA, Bonferroni post-hoc test p=0.2995)]. These results are illustrated in Figure 5C, D and Figure 6C, D.

In contrast to the small and transient increase in dendritic complexity caused by the T158M mutation, overexpression of wildtype *MECP2* did not affect dendritic complexity in CA3 pyramidal neurons after 2 days of transfection (WT *MECP2*, 5 cells from 4 slices, *vs*. eYFP, 13 cells from 7 slices; ANOVA, Bonferroni post-hoc test $p>0.05$; Fig. 5A, B) or 4 days of transfection (WT *MECP2*, 7 cells from 7 slices, *vs*. eYFP, 14 cells from 10 slices; ANOVA, Bonferroni post-hoc test $p>0.05$; Fig. 6A, B). Neither WT *MECP2* overexpression affected the total dendritic length after 2 days of transfection (WT *MECP2*= 2,675±742μm, *vs*. eYFP = 3,193±864μm; ANOVA, Bonferroni post-hoc test p=0.2559; Fig. 5D) or after 4 days of transfection (WT *MECP2* = 3131±665μm, *vs*. eYFP = 3,627±1048μm; ANOVA, Bonferroni post-hoc test p=0.2409; Fig. 6D). On the other hand, CA3 pyramidal neurons overexpressing WT *MECP2* showed fewer dendritic branch points after 2 days of transfection (WT *MECP2*

= 15.9±3.7 branch points, *vs*. eYFP = 23.6±7.5 branch points; ANOVA, Bonferroni post-hoc test p=0.0454; Fig. 5C). The latter effect was transient, since the total number of dendritic branch points was comparable in both groups after 4 days of expression (WT *MECP2* = 24.2 ±8.9 branch points, *vs*. eYFP = 23.7±8.6 branch points; ANOVA, Bonferroni post-hoc test p=0.8833; Fig. 6C).

Lastly, we investigated the consequences of endogenous *Mecp2* knockdown for dendritic complexity. After 2 days of expression, CA3 pyramidal neurons transfected with *MECP2*-specific shRNA showed significantly fewer dendritic branch points and shorter dendrites than control neurons [(*MECP2* shRNA = 22.3±8.4, *vs*. control shRNA = 40.8±17.9; ANOVA, Bonferroni post-hoc test p=0.0412) (*MECP2* shRNA = 2,923±809μm, *vs*. control shRNA = 4,669±1238μm; ANOVA, Bonferroni post-hoc test p=0.0133; Fig. 7A–D)]. However, this effect was transient, because the number of dendritic branch points and the total dendritic length after 4 days of *Mecp2* knockdown was comparable to those in control neurons [(*MECP2* shRNA = 4,506±1084μm, *vs*. control shRNA = 4,908±1182μm; ANOVA, Bonferroni post-hoc test p=0.634) (*MECP2* shRNA = 37.8±13.5 branch points, vs. control shRNA = 43.4±10 branch points; ANOVA, Bonferroni post-hoc test p=0.5283; Fig. 7E–H). On the other hand, the effects of *Mecp2* knockdown on dendritic complexity became evident only after 4 days of transfection. Dendritic complexity in CA3 pyramidal neurons was comparable in the two groups after 2 days of transfection (*MECP2* shRNA, 6 cells from 5 slices, *vs*. control shRNA, 7 cells from 6 slices; ANOVA, Bonferroni post-hoc test p>0.05; Fig. 7B), while it was significantly reduced – albeit only within the first 140μm of the apical dendritic tree – after 4 days of *Mecp2* knockdown (140μm from soma: *MECP2* shRNA 10.3±0.8 intersections, 4 cells from 4 slices, *vs*. control shRNA 18.5±1.4 intersections, 4 cells from 3 slices; ANOVA, Bonferroni post-hoc test p<0.05; Fig. 7F).

Discussion

Here, we present several novel observations regarding dendritic spine dysgenesis in RTT individuals and the role of the transcriptional regulator MeCP2 on dendritic complexity and dendritic spine density and morphology. First, we show that CA1 pyramidal neurons of the hippocampus in female individuals with RTT have lower dendritic spine density than age-matched unaffected (non-MR) female individuals, as observed qualitatively in pyramidal neurons of the motor cortex (Belichenko *et al*., 1994). Second, overexpression of *MECP2* missense mutations common in RTT patients (R106W or T158M) reduced dendritic spine density in hippocampal pyramidal neurons, particularly mature dendritic spines (i.e. mushroom and stubby types); on the other hand, overexpression of wildtype *MECP2* reduced spine density, but only transiently. It is important to note that the levels of the endogenous *Mecp2* gene were not manipulated in these experiments. Third, endogenous *Mecp2* knockdown also caused a reduction in dendritic spine density, especially of mature spines. Finally, overexpression of wildtype *MECP2* had a small effect on dendritic complexity, while knockdown of endogenous *Mecp2* transiently reduced dendritic length and branching in CA3 pyramidal neurons.

The brain pathology of RTT includes decreased neuronal size and increased cell density in numerous brain regions such as the cerebral cortex, hypothalamus, and the hippocampal formation (Bauman *et al*., 1995a; Bauman *et al*., 1995b). A decrease in dendritic branching and in the number of dendritic spines was reported in the cortex of individuals with RTT, or with a deletion of the *MECP2* gene (Armstrong *et al*., 1995; Belichenko *et al*., 1994; Schule *et al*., 2008). Furthermore, reduced levels of MAP-2, a dendritic protein involved in microtubule stabilization, were observed throughout the neocortex of RTT patients (Kaufmann *et al*., 2000; Kaufmann *et al*., 1995; Kaufmann *et al*., 1997a). COX-2, a protein enriched in dendritic spines, was also reduced in the cortex of RTT individuals (Kaufmann *et al*., 1997b).

We have extended those studies with quantitative analyses of dendritic spine density in apical secondary and tertiary dendrites of CA1 pyramidal neurons, which confirmed that RTT individuals have lower spine density than non-MR individuals. Intriguingly, glutamate receptor density has a differential distribution during RTT development, where younger individuals with RTT have a higher density compared to controls, while older individuals have a lower density compared to controls (Blue *et al*., 1999a; Blue *et al*., 1999b). The increase in glutamate receptor density may represent a homeostatic compensation for the reduction in dendritic spine density. On the other hand, the elevated glutamate levels measured in forebrain of RTT individuals by high-field strength MRI (Pan *et al*., 1999) may cause dendritic spine pruning (Segal *et al*., 2000).

Intriguingly, observations regarding neuronal and synaptic morphology in MeCP2-based models of Rett syndrome have produced varying results, sometimes inconsistent with the available information regarding the cellular neuropathology in RTT patients (Armstrong *et al*., 1995; Bauman *et al*., 1995a; Bauman *et al*., 1995b; Belichenko *et al*., 1994). However, it is important to note that no other study looked at the consequences of the expression of single-point mutants of *MECP2* on dendritic spine density in pyramidal neurons of the hippocampus, as we have done in the present study. Reduced excitatory synaptic transmission and plasticity in *Mecp2*-deficient mice have been interpreted to reflect a reduced number of excitatory synapses (Asaka *et al*., 2006; Chao *et al*., 2007; Dani *et al*., 2005). Fewer excitatory synapses may reflect delayed neuronal maturation, since newly generated granule cells in the dentate gyrus of *Mecp2* null mice have lower dendritic spine density than mature neighboring neurons (Smrt *et al*., 2007). Consistently, pyramidal neurons in the cortex of *Mecp2* null adult mice have reduced dendritic branching and spine density (Fukuda *et al*., 2005; Kishi and Macklis, 2004). A recent comprehensive study of the two available *Mecp2* null mouse models confirmed that granules cells of the dentate gyrus, and pyramidal neurons from hippocampal area CA1 and layers II-III of the motor cortex have lower dendritic spine densities than their control WT littermates (Belichenko *et al*. 2009a, b). In contrast, hippocampal and cortical neurons of transgenic knockin mice expressing a truncated *Mecp2* allele ($Mecp2^{308}$) – which recapitulate the RTT phenotype (Shahbazian *et al*., 2002a) – have dendritic, dendritic spine and excitatory synapse morphologies comparable to wildtype mice, despite significant impairments in hippocampal-dependent learning and memory and synaptic plasticity, interpreted as the consequence of the expression of a truncated non-functional MeCP2 protein (Moretti *et al*., 2006). On the other hand, duplications of the chromosomal region where *MECP2* is located in humans have been detected in neurological disorders associated with mental retardation (del Gaudio *et al*., 2006; Smyk *et al*., 2008). Intriguingly, transgenic mice that overexpress human *MECP2* at approximately twofold the endogenous MeCP2 protein levels have a higher learning rate of hippocampal-dependent tasks and enhanced in hippocampal synaptic plasticity, though they develop seizures after 20 weeks of age, and death occurs shortly thereafter (Collins *et al*., 2004). The physiological and behavioral phenotypes in *MECP2* overexpressing mice may result from a higher density of excitatory synapses compared to wildtype littermates (Chao *et al*., 2007). Surprisingly, overexpression of wildtype *Mecp2* reaching ~4–5 fold the endogenous levels reduced dendritic branching and increased the length of dendritic spines of hippocampal pyramidal neurons, without affecting spine density (Zhou *et al*., 2006). It is relevant to note that the latter studies had to overexpress the anti-apoptotic protein Bcl-XL to prevent neuronal cell death caused by *Mecp2* overexpression at such high levels (Zhou *et al*., 2006). Incidentally, overexpression of Bcl-XL by itself increased the number of excitatory synapses between cultured hippocampal neurons (Li *et al*., 2008). The apparent discrepancies with earlier observations made in other experimental systems may originate from different developmental stages (*in vivo* development *vs*. 10 days *in vitro* organotypic slice cultures from P7 hippocampal slices), duration of expression of either a non-functional truncated MeCP2 protein (several weeks expression *in vivo*) or single-point mutants with reduced activity (4 days expression *in vitro*), and analyses of Golgi-stained sections by brightfield microscopy *vs*. individually-

labeled neurons by laser-scanning confocal microscopy. It is important to note that, for the purposes of this study, we pooled dendritic spine densities from secondary and tertiary apical dendrites of CA1 and CA3 neurons, which received the same presynaptic input from CA3 neurons (reviewed in Spruston and McBain, 2007). Statistical comparisons confirmed that spine density was not significantly different between the imaged CA1 and CA3 dendrites in none of the experimental groups, including after *MECP2/Mecp2* manipulations. Of relevance to RTT, where mutant forms of MeCP2 are expressed in a mosaic fashion due to X chromosome inactivation, the "spotted" transfection of RTT-associated *MECP2* mutations yielded by particle-mediated gene transfer in hippocampal slice cultures resulted in a more dramatic dendritic spine loss than the shRNA-mediated knockdown of the endogenous MeCP2 protein expression.

Considering the direct relationship between the morphology of dendritic spines and the maturation state and strength of excitatory synapses on them (reviewed by Kasai *et al*., 2003; Nimchinsky *et al*., 2002; Yuste *et al*., 2000), it is consistent that overexpression of RTT-associated *MECP2* mutations cause a selective loss of mature dendritic spines, i.e. stubby and mushroom types (Boda *et al*., 2004; Tyler and Pozzo-Miller, 2003; reviewed by Chapleau and Pozzo-Miller, 2007; Harris, 1999). Since larger spines (including stubby and mushroom spines) are the postsynaptic compartment of excitatory synapses that are stronger than those formed onto thin spines, as estimated by the amplitude of AMPAR-mediated postsynaptic currents (Matsuzaki *et al*., 2001; Matsuzaki *et al*., 2004), a lower density of morphologically mature spines suggests that overexpression of RTT-associated *MECP2* mutations or endogenous *Mecp2* knockdown reduce the strength of excitatory synapses. Such weakening of excitatory synaptic strength may precede spine and synapse shrinkage and pruning (Bastrikova *et al*., 2008; Becker *et al*., 2008; Segal *et al*., 2000; Zhou *et al*., 2004).

Lastly, our observations indicate the importance of MeCP2 expression levels for the maintenance of dendritic tree structure. Indeed, wildtype *MECP2* overexpression or endogenous *Mecp2* knockdown reduced the branching of apical dendrites, as previously shown (Zhou *et al*., 2006). However, the overexpression of mutant *MECP2* caused the opposite effect, increasing dendritic complexity. Since the overexpression of mutant *MECP2* causes a significant loss in the total number of spines, especially of mature spines, the enhancement in dendritic complexity might reflect a compensatory homeostatic mechanism in the face of significant loss of mature excitatory synapses.

In summary, we have presented evidence in support of a cell-autonomous role of MeCP2 levels in the maintenance of mature dendritic spines and the complexity of the dendritic tree of postnatal pyramidal neurons within an established neuronal network. The mutations in the methyl-binding domain of MeCP2 used in our studies (R106W and T158M) were shown to reduce its binding to methyl-CpG-dinucleotides, impairing its transcriptional repression of a reporter gene (Ballestar *et al*., 2000; Ghosh *et al*., 2008; Kudo *et al*., 2001; Kudo *et al*., 2003; Yusufzai and Wolffe, 2000). Recently, a gene profiling study identified 2,582 genes symmetrically misregulated in the hypothalamus of *Mecp2* null and *MECP2* overexpressing mice, suggesting that they represent primary targets (Chahrour *et al*., 2008). Unexpectedly, 85% of them seem to be activated by MeCP2 based on the fact that they were up-regulated in *MECP2* overexpressing mice and down-regulated in *Mecp2* null mice. It remains unknown whether RTT-causing mutations affect MeCP2's role in transcriptional activation, repression or both. Taken together, our results demonstrate reduced density of dendritic spines – the postsynaptic element of excitatory synapses – in CA1 pyramidal neurons of the hippocampus of individuals with RTT, a distinct dendritic phenotype that is recapitulated in post-mitotic neurons expressing RTT-associated *MECP2* mutations or after shRNA-mediated endogenous *Mecp2* knockdown, suggesting that this phenotype represents a cell-autonomous consequence of MeCP2 dysfunction.

Supplementary Material

Refer to Web version on PubMed Central for supplementary material.

Acknowledgements

Supported by NIH grants NS40593 and NS057780, IRSF and the Civitan International Foundation (LP-M). We also thank the assistance of the UAB Intellectual and Developmental Disabilities Research Center (IDDRC; P30-HD38985) and the UAB Neuroscience Cores (P30-NS47466, P30-NS57098). Human tissue was obtained from the NICHD Brain and Tissue Bank for Developmental Disorders at the University of Maryland, Baltimore, MD. We thank Dr. Carolyn Schanen (Nemours Biomedical Research, Alfred I. duPont Hospital for Children, Wilmington, DE, USA), and Mr. J. Matthew Rutherford for discussions and comments on the manuscript. We also thank Dr. Mark Beasley for statistical analyses (IDDRC Biometry Core A; UAB School of Public Health, Biostatistics).

REFERENCES

Akbarian S, Chen RZ, Gribnau J, Rasmussen TP, Fong H, Jaenisch R, Jones EG. Expression pattern of the Rett syndrome gene MeCP2 in primate prefrontal cortex. Neurobiol Dis 2001;8:784–791. [PubMed: 11592848]

Alonso M, Medina JH, Pozzo-Miller L. ERK1/2 activation is necessary for BDNF to increase dendritic spine density in hippocampal CA1 pyramidal neurons. Learn Mem 2004;11:172–178. [PubMed: 15054132]

Amir RE, Van den Veyver IB, Wan M, Tran CQ, Francke U, Zoghbi HY. Rett syndrome is caused by mutations in X-linked MECP2, encoding methyl-CpG-binding protein 2. Nat Genet 1999;23:185–188. [PubMed: 10508514]

Armstrong D, Dunn JK, Antalffy B, Trivedi R. Selective dendritic alterations in the cortex of Rett syndrome. J Neuropathol Exp Neurol 1995;54:195–201. [PubMed: 7876888]

Asaka Y, Jugloff DG, Zhang L, Eubanks JH, Fitzsimonds RM. Hippocampal synaptic plasticity is impaired in the Mecp2-null mouse model of Rett syndrome. Neurobiol Dis 2006;21:217–227. [PubMed: 16087343]

Ballestar E, Yusufzai TM, Wolffe AP. Effects of Rett syndrome mutations of the methyl-CpG binding domain of the transcriptional repressor MeCP2 on selectivity for association with methylated DNA. Biochemistry 2000;39:7100–7106. [PubMed: 10852707]

Bastrikova N, Gardner GA, Reece JM, Jeromin A, Dudek SM. Synapse elimination accompanies functional plasticity in hippocampal neurons. Proc Natl Acad Sci U S A 2008;105:3123–3127. [PubMed: 18287055]

Bauman ML, Kemper TL, Arin DM. Microscopic observations of the brain in Rett syndrome. Neuropediatrics 1995a;26:105–108. [PubMed: 7566446]

Bauman ML, Kemper TL, Arin DM. Pervasive neuroanatomic abnormalities of the brain in three cases of Rett's syndrome. Neurology 1995b;45:1581–1586. [PubMed: 7644058]

Becker N, Wierenga CJ, Fonseca R, Bonhoeffer T, Nagerl UV. LTD induction causes morphological changes of presynaptic boutons and reduces their contacts with spines. Neuron 2008;60:590–597. [PubMed: 19038217]

Belichenko NP, Belichenko PV, Mobley WC. Evidence for both neuronal cell autonomous and nonautonomous effects of methyl-CpG-binding protein 2 in the cerebral cortex of female mice with *Mecp2* mutation. Neurobiol Dis 2009a;34:71–77. [PubMed: 19167498]

Belichenko PV, Oldfors A, Hagberg B, Dahlstrom A. Rett syndrome: 3-D confocal microscopy of cortical pyramidal dendrites and afferents. Neuroreport 1994;5:1509–1513. [PubMed: 7948850]

Belichenko PV, Wright EE, Belichenko NP, Masliah E, Li HH, Mobley WC, Francke U. Widespread changes in dendritic and axonal morphology in *Mecp2*-mutant mouse models of Rett syndrome: evidence for disruption of neuronal networks. J Comp Neurol 2009b;514:240–258. [PubMed: 19296534]

Blue ME, Naidu S, Johnston MV. Altered development of glutamate and GABA receptors in the basal ganglia of girls with Rett syndrome. Exp Neurol 1999a;156:345–352. [PubMed: 10328941]

Blue ME, Naidu S, Johnston MV. Development of amino acid receptors in frontal cortex from girls with Rett syndrome. Ann Neurol 1999b;45:541–545. [PubMed: 10211484]

Boda B, Alberi S, Nikonenko I, Node-Langlois R, Jourdain P, Moosmayer M, Parisi-Jourdain L, Muller D. The mental retardation protein PAK3 contributes to synapse formation and plasticity in hippocampus. J Neurosci 2004;24:10816–10825. [PubMed: 15574732]

Cassel S, Revel MO, Kelche C, Zwiller J. Expression of the methyl-CpG-binding protein MeCP2 in rat brain. An ontogenetic study. Neurobiol Dis 2004;15:206–211.

Chahrour M, Jung SY, Shaw C, Zhou X, Wong ST, Qin J, Zoghbi HY. MeCP2, a Key Contributor to Neurological Disease, Activates and Represses Transcription. Science 2008;320:1224–1229. [PubMed: 18511691]

Chao HT, Zoghbi HY, Rosenmund C. MeCP2 controls excitatory synaptic strength by regulating glutamatergic synapse number. Neuron 2007;56:58–65. [PubMed: 17920015]

Chapleau, CA.; Pozzo-Miller, L. Activity-dependent structural plasticity of dendritic spines. In: Byrne, J., editor. Learning and Memory: a Comprehensive Reference. Vol. Volume 4. Oxford: Elsevier; 2007. p. 695-719.

Collins AL, Levenson JM, Vilaythong AP, Richman R, Armstrong DL, Noebels JL, David Sweatt J, Zoghbi HY. Mild overexpression of MeCP2 causes a progressive neurological disorder in mice. Hum Mol Genet 2004;13:2679–2689. [PubMed: 15351775]

Couvert P, Bienvenu T, Aquaviva C, Poirier K, Moraine C, Gendrot C, Verloes A, Andres C, Le Fevre AC, Souville I, Steffann J, des Portes V, Ropers HH, Yntema HG, Fryns JP, Briault S, Chelly J, Cherif B. MECP2 is highly mutated in X-linked mental retardation. Hum Mol Genet 2001;10:941–946. [PubMed: 11309367]

Dani VS, Chang Q, Maffei A, Turrigiano GG, Jaenisch R, Nelson SB. Reduced cortical activity due to a shift in the balance between excitation and inhibition in a mouse model of Rett syndrome. Proc Natl Acad Sci U S A 2005;102:12560–12565. [PubMed: 16116096]

del Gaudio D, Fang P, Scaglia F, Ward PA, Craigen WJ, Glaze DG, Neul JL, Patel A, Lee JA, Irons M, Berry SA, Pursley AA, Grebe TA, Freedenberg D, Martin RA, Hsich GE, Khera JR, Friedman NR, Zoghbi HY, Eng CM, Lupski JR, Beaudet AL, Cheung SW, Roa BB. Increased MECP2 gene copy number as the result of genomic duplication in neurodevelopmentally delayed males. Genet Med 2006;8:784–792. [PubMed: 17172942]

Erdfelder E, Faul F, Buchner A. GPOWER: A general power analysis program. Behavior Research Methods 1996;28:1–11.

Fiala JC, Spacek J, Harris KM. Dendritic spine pathology: cause or consequence of neurological disorders? Brain Res Brain Res Rev 2002;39:29–54. [PubMed: 12086707]

Fukuda T, Itoh M, Ichikawa T, Washiyama K, Goto Y. Delayed maturation of neuronal architecture and synaptogenesis in cerebral cortex of Mecp2-deficient mice. J Neuropathol Exp Neurol 2005;64:537–544. [PubMed: 15977646]

Gan WB, Grutzendler J, Wong WT, Wong RO, Lichtman JW. Multicolor "DiOlistic" labeling of the nervous system using lipophilic dye combinations. Neuron 2000;27:219–225. [PubMed: 10985343]

Gemelli T, Berton O, Nelson ED, Perrotti LI, Jaenisch R, Monteggia LM. Postnatal loss of methyl-CpG binding protein 2 in the forebrain is sufficient to mediate behavioral aspects of Rett syndrome in mice. Biol Psychiatry 2006;59:468–476. [PubMed: 16199017]

Ghosh RP, Horowitz-Scherer RA, Nikitina T, Gierasch LM, Woodcock CL. Rett syndrome-causing mutations in human MeCP2 result in diverse structural changes that impact folding and DNA interactions. J Biol Chem 2008;283:20523–20534. [PubMed: 18499664]

Harris KM. Structure, development, and plasticity of dendritic spines. Curr Opin Neurobiol 1999;9:343–348. [PubMed: 10395574]

Ho KL, McNae IW, Schmiedeberg L, Klose RJ, Bird AP, Walkinshaw MD. MeCP2 binding to DNA depends upon hydration at methyl-CpG. Mol Cell 2008;29:525–531. [PubMed: 18313390]

Huttenlocher PR. Dendritic development and mental defect. Neurology 1970;20:381. [PubMed: 5534993]

Huttenlocher PR. Dendritic development in neocortex of children with mental defect and infantile spasms. Neurology 1974;24:203–210. [PubMed: 4130661]

Jugloff DG, Jung BP, Purushotham D, Logan R, Eubanks JH. Increased dendritic complexity and axonal length in cultured mouse cortical neurons overexpressing methyl-CpG-binding protein MeCP2. Neurobiol Dis 2005;19:18–27. [PubMed: 15837557]

Jung BP, Jugloff DG, Zhang G, Logan R, Brown S, Eubanks JH. The expression of methyl CpG binding factor MeCP2 correlates with cellular differentiation in the developing rat brain and in cultured cells. J Neurobiol 2003;55:86–96. [PubMed: 12605461]

Kankirawatana P, Leonard H, Ellaway C, Scurlock J, Mansour A, Makris CM, Dure LSt, Friez M, Lane J, Kiraly-Borri C, Fabian V, Davis M, Jackson J, Christodoulou J, Kaufmann WE, Ravine D, Percy AK. Early progressive encephalopathy in boys and MECP2 mutations. Neurology 2006;67:164–166. [PubMed: 16832102]

Kasai H, Matsuzaki M, Noguchi J, Yasumatsu N, Nakahara H. Structure-stability-function relationships of dendritic spines. Trends Neurosci 1987;26:360–368. [PubMed: 12850432]

Katz LC. Local circuitry of identified projection neurons in cat visual cortex brain slices. J Neurosci 1987;7:1223–1249. [PubMed: 3553446]

Kaufmann WE, Johnston MV, Blue ME. MeCP2 expression and function during brain development: implications for Rett syndrome's pathogenesis and clinical evolution. Brain Dev 2005;27:S77–S87. [PubMed: 16182491]

Kaufmann WE, MacDonald SM, Altamura CR. Dendritic cytoskeletal protein expression in mental retardation: an immunohistochemical study of the neocortex in Rett syndrome. Cereb Cortex 2000;10:992–1004. [PubMed: 11007550]

Kaufmann WE, Moser HW. Dendritic anomalies in disorders associated with mental retardation. Cereb Cortex 2000;10:981–991. [PubMed: 11007549]

Kaufmann WE, Naidu S, Budden S. Abnormal expression of microtubule-associated protein 2 (MAP-2) in neocortex in Rett syndrome. Neuropediatrics 1995;26:109–113. [PubMed: 7566447]

Kaufmann WE, Taylor CV, Hohmann CF, Sanwal IB, Naidu S. Abnormalities in neuronal maturation in Rett syndrome neocortex: preliminary molecular correlates. Eur Child Adolesc Psychiatry 1997a; 6:75–77. [PubMed: 9452926]

Kaufmann WE, Worley PF, Taylor CV, Bremer M, Isakson PC. Cyclooxygenase-2 expression during rat neocortical development and in Rett syndrome. Brain Dev 1997b;19:25–34. [PubMed: 9071487]

Kishi N, Macklis JD. MECP2 is progressively expressed in post-migratory neurons and is involved in neuronal maturation rather than cell fate decisions. Mol Cell Neurosci 2004;27:306–321. [PubMed: 15519245]

Kudo S. Methyl-CpG-binding protein MeCP2 represses Sp1-activated transcription of the human leukosialin gene when the promoter is methylated. Mol Cell Biol 1998;18:5492–5499. [PubMed: 9710633]

Kudo S, Nomura Y, Segawa M, Fujita N, Nakao M, Dragich J, Schanen C, Tamura M. Functional analyses of MeCP2 mutations associated with Rett syndrome using transient expression systems. Brain Dev 2001;23:S165–S173. [PubMed: 11738866]

Kudo S, Nomura Y, Segawa M, Fujita N, Nakao M, Schanen C, Tamura M. Heterogeneity in residual function of MeCP2 carrying missense mutations in the methyl CpG binding domain. J Med Genet 2003;40:487–493. [PubMed: 12843318]

Larimore J, Chapleau CA, Kudo S, Theibert A, Percy AK, Pozzo-Miller L. *Bdnf* overexpression in hippocampal neurons prevents dendritic atrophy caused by Rett-associated *MECP2* mutations. Neurobiol Dis 2009;34:199–211. [PubMed: 19217433]

Li H, Chen Y, Jones AF, Sanger RH, Collis LP, Flannery R, McNay EC, Yu T, Schwarzenbacher R, Bossy B, Bossy-Wetzel E, Bennett MV, Pypaert M, Hickman JA, Smith PJ, Hardwick JM, Jonas EA. Bcl-xL induces Drp1-dependent synapse formation in cultured hippocampal neurons. Proc Natl Acad Sci U S A 2008;105:2169–2174. [PubMed: 18250306]

Marin-Padilla M. Structural abnormalities of the cerebral cortex in human chromosomal aberrations: a Golgi study. Brain Res 1972;44:625–629. [PubMed: 4263073]

Marin-Padilla M. Pyramidal cell abnormalities in the motor cortex of a child with Down's syndrome. A Golgi study. J Comp Neurol 1976;167:63–81.

Masuyama T, Matsuo M, Jing JJ, Tabara Y, Kitsuki K, Yamagata H, Kan Y, Miki T, Ishii K, Kondo I. Classic Rett syndrome in a boy with R133C mutation of MECP2. Brain Dev 2005;27:439–442. [PubMed: 16122633]

Matsuzaki M, Ellis-Davies GC, Nemoto T, Miyashita Y, Iino M, Kasai H. Dendritic spine geometry is critical for AMPA receptor expression in hippocampal CA1 pyramidal neurons. Nat Neurosci 2001;4:1086–1092. [PubMed: 11687814]

Matsuzaki M, Honkura N, Ellis-Davies GC, Kasai H. Structural basis of long-term potentiation in single dendritic spines. Nature 2004;429:761–766. [PubMed: 15190253]

Moog U, Smeets EE, van Roozendaal KE, Schoenmakers S, Herbergs J, Schoonbrood-Lenssen AM, Schrander-Stumpel CT. Neurodevelopmental disorders in males related to the gene causing Rett syndrome in females (MECP2). Eur J Paediatr Neurol 2003;7:5–12. [PubMed: 12615169]

Moore CD, Thacker EE, Larimore J, Gaston D, Underwood A, Kearns B, Patterson SI, Jackson T, Chapleau C, Pozzo-Miller L, Theibert A. The neuronal Arf GAP centaurin alpha1 modulates dendritic differentiation. J Cell Sci 2007;120:2683–2693. [PubMed: 17635995]

Moretti P, Levenson JM, Battaglia F, Atkinson R, Teague R, Antalffy B, Armstrong D, Arancio O, Sweatt JD, Zoghbi HY. Learning and memory and synaptic plasticity are impaired in a mouse model of Rett syndrome. J Neurosci 2006;26:319–327. [PubMed: 16399702]

Mullaney BC, Johnston MV, Blue ME. Developmental expression of methyl-CpG binding protein 2 is dynamically regulated in the rodent brain. Neuroscience 2004;123:939–949. [PubMed: 14751287]

Nelson ED, Kavalali ET, Monteggia LM. MeCP2-dependent transcriptional repression regulates excitatory neurotransmission. Curr Biol 2006;16:710–716. [PubMed: 16581518]

Nimchinsky EA, Sabatini BL, Svoboda K. Structure and function of dendritic spines. Annu Rev Physiol 2002;64:313–353. [PubMed: 11826272]

Pan JW, Lane JB, Hetherington H, Percy AK. Rett syndrome: 1H spectroscopic imaging at 4.1 Tesla. J Child Neurol 1999;14:524–528. [PubMed: 10456763]

Percy AK. Rett syndrome: clinical correlates of the newly discovered gene. Brain Dev 2001;23:S202–S205. [PubMed: 11738873]

Percy AK, Lane JB. Rett syndrome: model of neurodevelopmental disorders. J Child Neurol 2005;20:718–721. [PubMed: 16225824]

Peters, A.; Palay, SL.; Webster, H. Neurons and Their Supporting Cells. New York: Oxford University Press; 1991. The Fine Structure of the Nervous System.

Purpura DP. Dendritic spine "dysgenesis" and mental retardation. Science 1974;186:1126–1128. [PubMed: 4469701]

Schule B, Armstrong D, Vogel H, Oviedo A, Francke U. Severe congenital encephalopathy caused by MECP2 null mutations in males: central hypoxia and reduced neuronal dendritic structure. Clin Genet 2008;74:116–126. [PubMed: 18477000]

Segal I, Korkotian I, Murphy DD. Dendritic spine formation and pruning: common cellular mechanisms? Trends Neurosci 2000;23:53–57. [PubMed: 10652540]

Shahbazian M, Young J, Yuva-Paylor L, Spencer C, Antalffy B, Noebels J, Armstrong D, Paylor R, Zoghbi H. Mice with truncated MeCP2 recapitulate many Rett syndrome features and display hyperacetylation of histone H3. Neuron 2002a;35:243–254. [PubMed: 12160743]

Shahbazian MD, Antalffy B, Armstrong DL, Zoghbi HY. Insight into Rett syndrome: MeCP2 levels display tissue- and cell-specific differences and correlate with neuronal maturation. Hum Mol Genet 2002b;11:115–124. [PubMed: 11809720]

Sholl DA. Dendritic organization in the neurons of the visual and motor cortices of the cat. J Anat 1953;87:387–406. [PubMed: 13117757]

Smrt RD, Eaves-Egenes J, Barkho BZ, Santistevan NJ, Zhao C, Aimone JB, Gage FH, Zhao X. Mecp2 deficiency leads to delayed maturation and altered gene expression in hippocampal neurons. Neurobiol Dis 2007;27:77–89. [PubMed: 17532643]

Smyk M, Obersztyn E, Nowakowska B, Nawara M, Cheung SW, Mazurczak T, Stankiewicz P, Bocian E. Different-sized duplications of Xq28, including MECP2, in three males with mental retardation, absent or delayed speech, and recurrent infections. Am J Med Genet B Neuropsychiatr Genet 147B 2008:799–806.

Spruston, N.; McBain, C. Andersen, P.; Morris, R.; Amaral, D.; Bliss, T.; O'Keefe, J. The Hippocampus Book. New York: Oxford University Press; 2007. Structural and functional properties of hippocampal neurons.

Stoppini L, Buchs PA, Muller D. A simple method for organotypic cultures of nervous tissue. J Neurosci Methods 1991;37:173–182. [PubMed: 1715499]

Tyler WJ, Pozzo-Miller L. Miniature synaptic transmission and BDNF modulate dendritic spine growth and form in rat CA1 neurones. J Physiol 2003;553:497–509. [PubMed: 14500767]

Yuste R, Majewska A, Holthoff K. From form to function: calcium compartmentalization in dendritic spines. Nat Neurosci 2000;3:653–659. [PubMed: 10862697]

Yusufzai TM, Wolffe AP. Functional consequences of Rett syndrome mutations on human MeCP2. Nucleic Acids Res 2000;28:4172–4179. [PubMed: 11058114]

Zhou Q, Homma KJ, Poo MM. Shrinkage of dendritic spines associated with long-term depression of hippocampal synapses. Neuron 2004;44:749–757. [PubMed: 15572107]

Zhou Z, Hong EJ, Cohen S, Zhao WN, Ho HY, Schmidt L, Chen WG, Lin Y, Savner E, Griffith EC, Hu L, Steen JA, Weitz CJ, Greenberg ME. Brain-specific phosphorylation of MeCP2 regulates activity-dependent Bdnf transcription, dendritic growth, and spine maturation. Neuron 2006;52:255–269. [PubMed: 17046689]

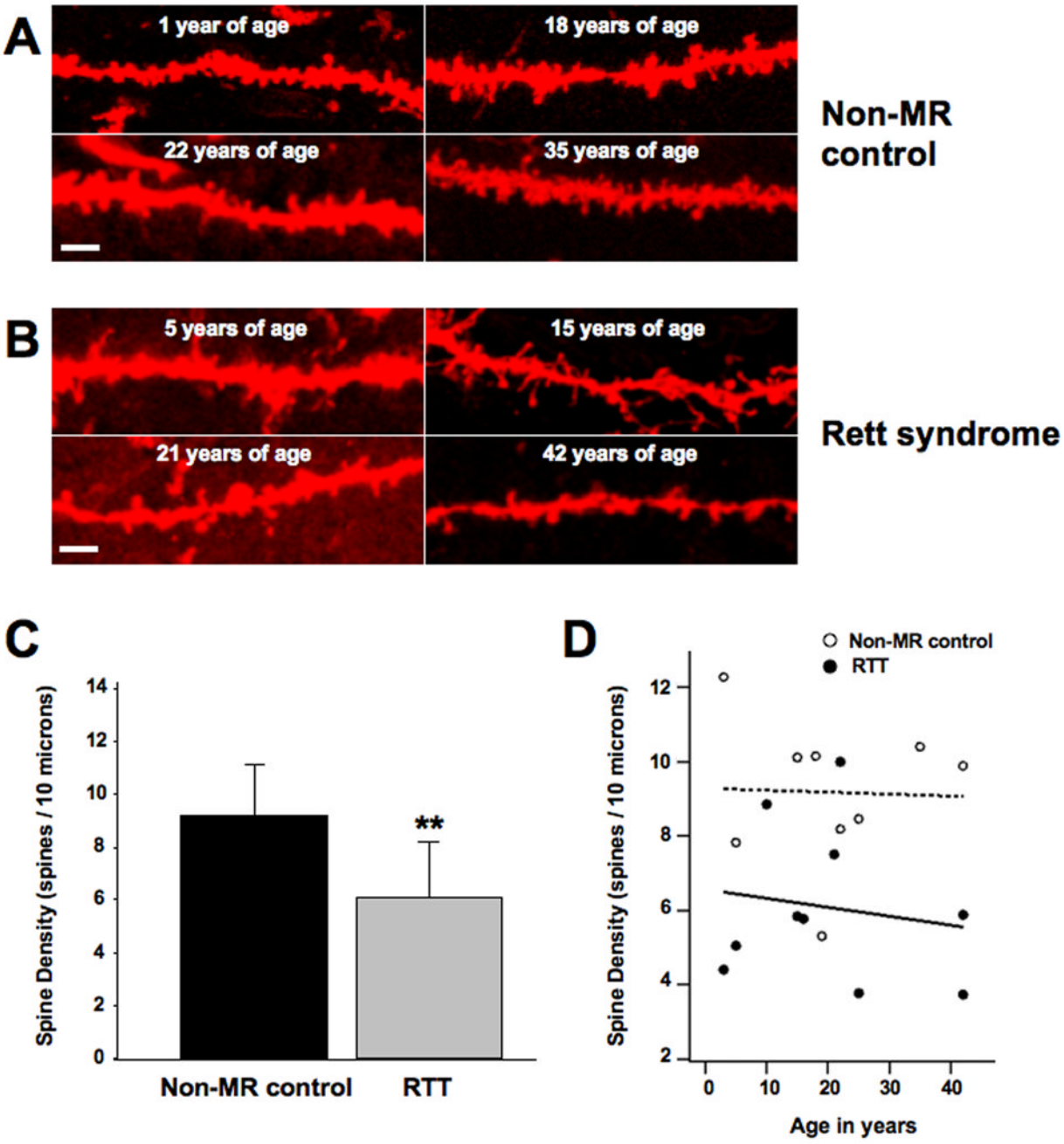

FIGURE 1. QUANTITATIVE ANALYSIS IN HUMAN POSTMORTEM BRAIN HIPPOCAMPUS REVEALS THAT CA1 PYRAMIDAL NEURONS OF RTT INDIVIDUALS HAVE LOWER DENDRITIC SPINE DENSITY THAN THOSE OF NON-MR INDIVIDUALS

Formalin-fixed human brain samples were obtained from the Harvard Brain Bank and from the University of Maryland Brain Bank (Table 1 contains all available information on the individuals whose brains were used in this study). **A.** Representative examples of DiI-stained secondary and tertiary apical dendritic segments of CA1 pyramidal neurons from unaffected (non-MR) female individuals who served as controls. **B.** Representative examples of DiI-stained secondary and tertiary apical dendritic segments of CA1 pyramidal neurons from female RTT individuals. **C.** Dendritic spine density expressed per 10μm of dendritic length.

D. Least square regression analyses of correlation between age and spine density in controls and RTT neurons. In this and all subsequent figures, data are presented as mean±SD, and * indicates $p<0.05$, ** indicates $p<0.01$, and *** indicates $p<0.001$, after unpaired two-tailed Student's t test (see text for details). In this and all subsequent figures, scale bar represents 2μm.

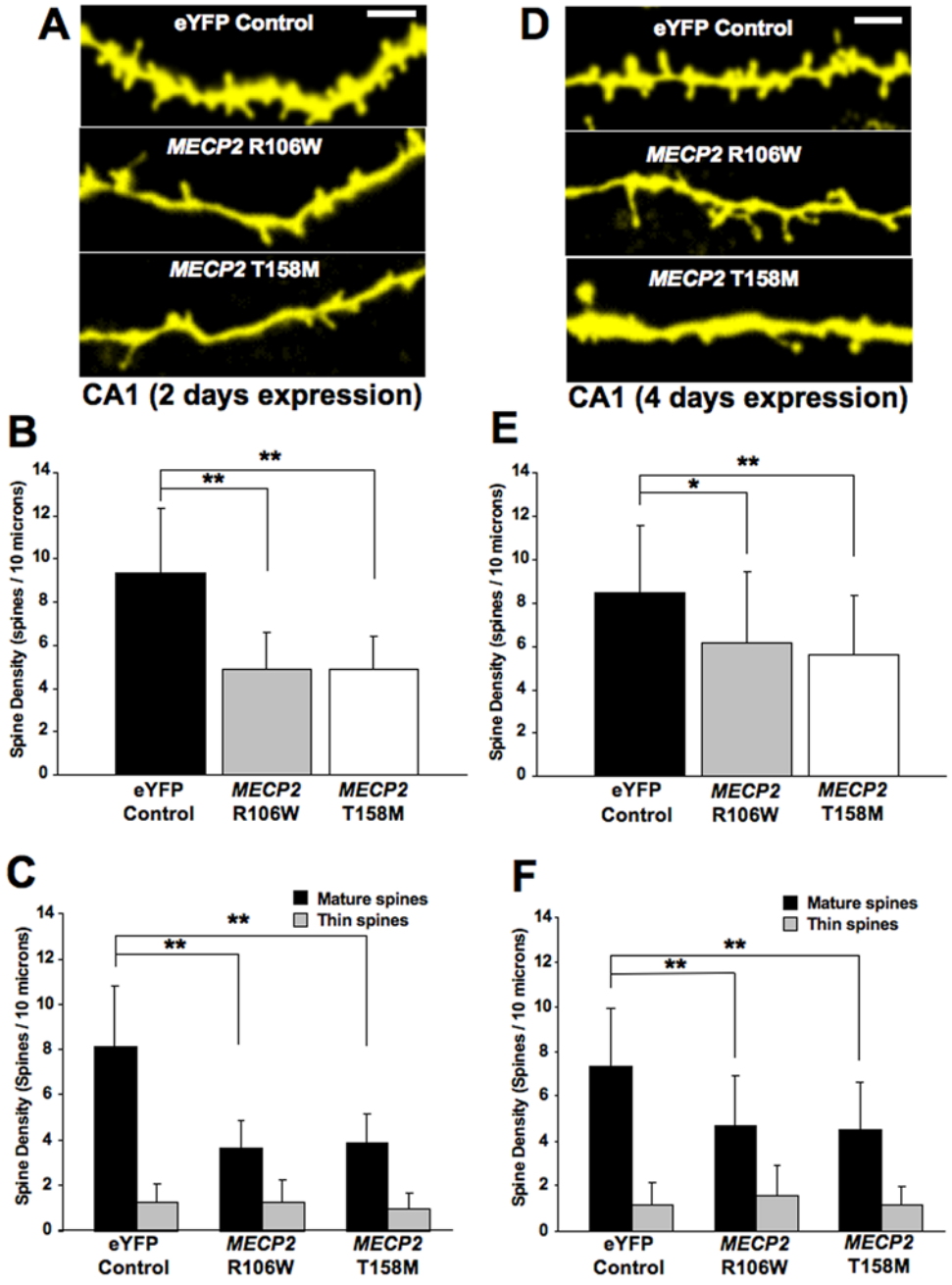

FIGURE 2. OVEREXPRESSION OF RTT-ASSOCIATED *MECP2* MUTATIONS CAUSES A PERSISTENT REDUCTION IN DENDRITIC SPINE DENSITY IN HIPPOCAMPAL PYRAMIDAL NEURONS

A. Representative examples of apical secondary or tertiary dendritic segments of CA1 pyramidal neurons expressing either an eYFP control plasmid or expression plasmids encoding GFP-tagged mutations in the methyl-binding domain of the MeCP2 (R106W or T158M) after 2 days of expression. **B.** Dendritic spine density expressed per 10μm of dendritic length. **C.** Density of each morphological type of dendritic spine (see text for classification criterion). **D.** Representative examples of apical secondary or tertiary dendritic segments of CA1 pyramidal neurons expressing either the eYFP control plasmid or mutant *MECP2* after 4 days

of expression). **E.** Dendritic spine density expressed per 10μm of dendritic length. **F.** Density of each morphological type of dendritic spine.

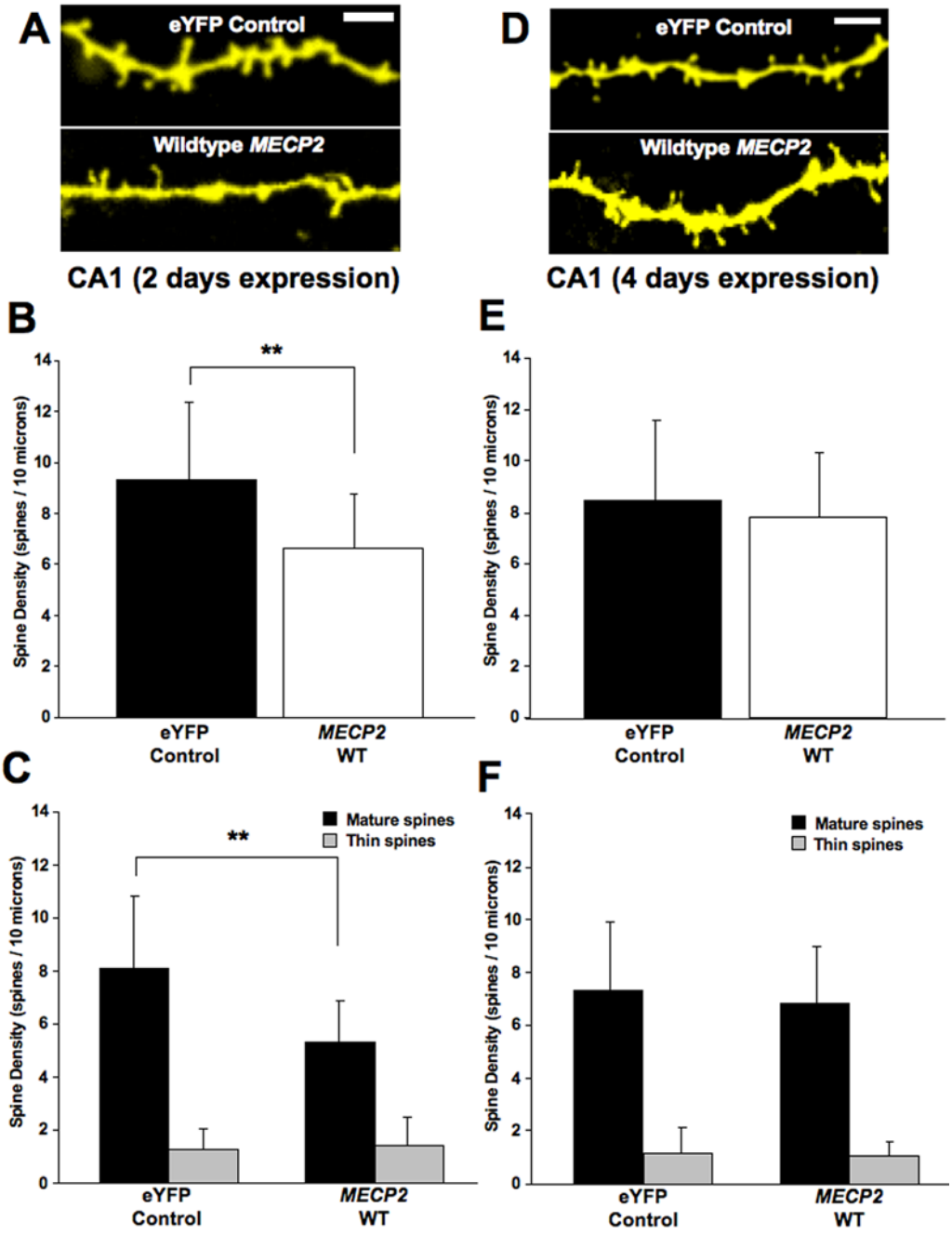

FIGURE 3. OVEREXPRESSION OF WILDTYPE *MECP2* CAUSES A TRANSIENT REDUCTION IN DENDRITIC SPINE DENSITY IN HIPPOCAMPAL PYRAMIDAL NEURONS

A. Representative examples of apical secondary or tertiary dendritic segments of pyramidal neurons expressing either the eYFP control plasmid or wildtype *MECP2* after 2 days of expression. **B.** Dendritic spine density expressed per 10μm of dendritic length. **C.** Density of each morphological type of dendritic spine. **D.** Representative examples of apical secondary or tertiary dendritic segments of CA1 pyramidal neurons expressing either the eYFP control plasmid or wildtype *MECP2* after 4 days of expression. **E.** Dendritic spine density expressed per 10μm of dendritic length. **F.** Density of each morphological type of dendritic spine.

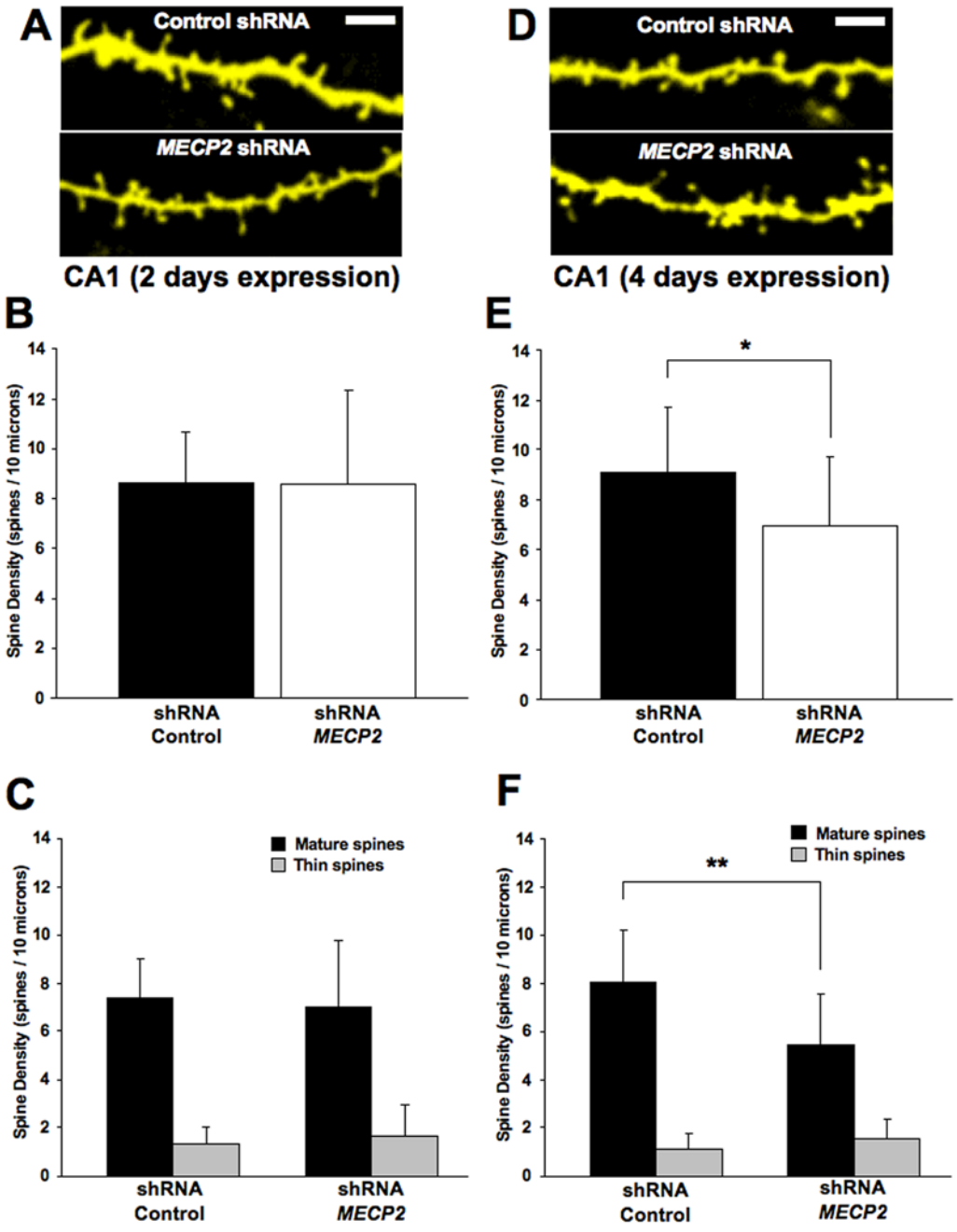

FIGURE 4. KNOCKDOWN OF ENDOGENOUS *MECP2* CAUSES A REDUCTION IN THE DENSITY OF MATURE DENDRITIC SPINES ONLY AFTER 4 DAYS OF TRANSFECTION

A. Representative examples of apical secondary or tertiary dendritic segments of CA1 pyramidal neurons expressing either the eYFP control plasmid or an shRNA interfering sequence to knockdown endogenous *Mecp2* after 2 days of expression. **B.** Dendritic spine density expressed per 10μm of dendritic length. **C.** Density of each morphological type of dendritic spine. **D.** Representative examples of apical secondary or tertiary dendritic segments of CA1 pyramidal neurons expressing either the eYFP control plasmid or an shRNA interfering sequence to knockdown endogenous *Mecp2* after 4 days of expression. **E.** Dendritic spine

density expressed per 10μm of dendritic length. **F.** Density of each morphological type of dendritic spine.

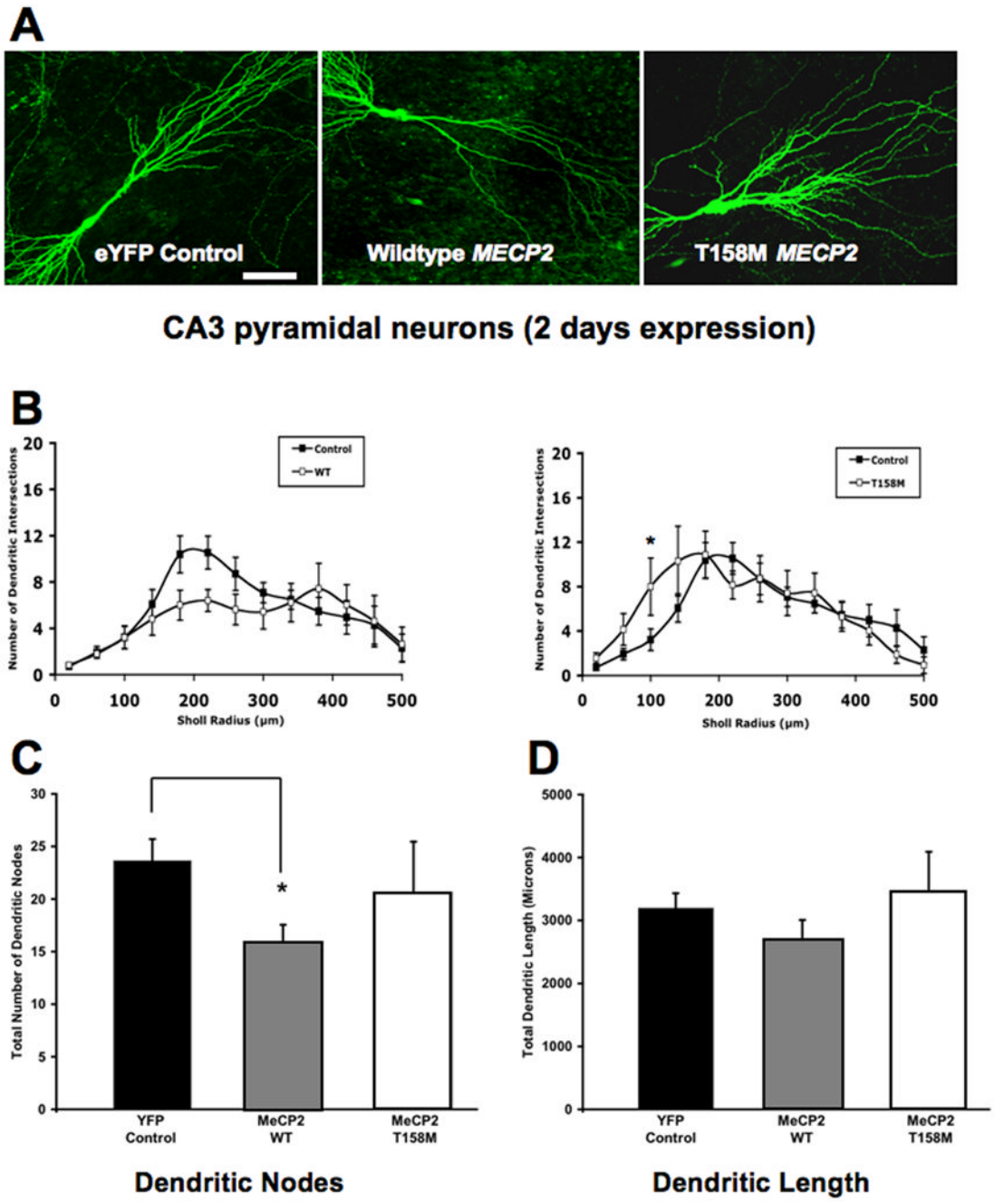

FIGURE 5. OVEREXPRESSION OF WILDTYPE *MECP2* TRANSIENTLY REDUCES THE NUMBER OF DENDRITIC NODES AND THE TOTAL DENDRITIC LENGTH, WHILE T158M *MECP2* TRANSIENTLY INCREASES DENDRITIC COMPLEXITY (2 DAYS OF EXPRESSION)

A. Representative low magnification views of eYFP-expressing CA3 pyramidal neurons transfected with either wildtype *MECP2* or the T158M *MECP2* mutant (2 days of expression). **B.** Three-dimensional Sholl analysis of dendritic complexity. Total number of intersections of CA3 apical dendrites as a function of distance from the soma. **C.** Total number of apical dendritic nodes. **D.** Total dendritic length. In this and Figure 6 and Figure 7, the scale bar represents 50μm.

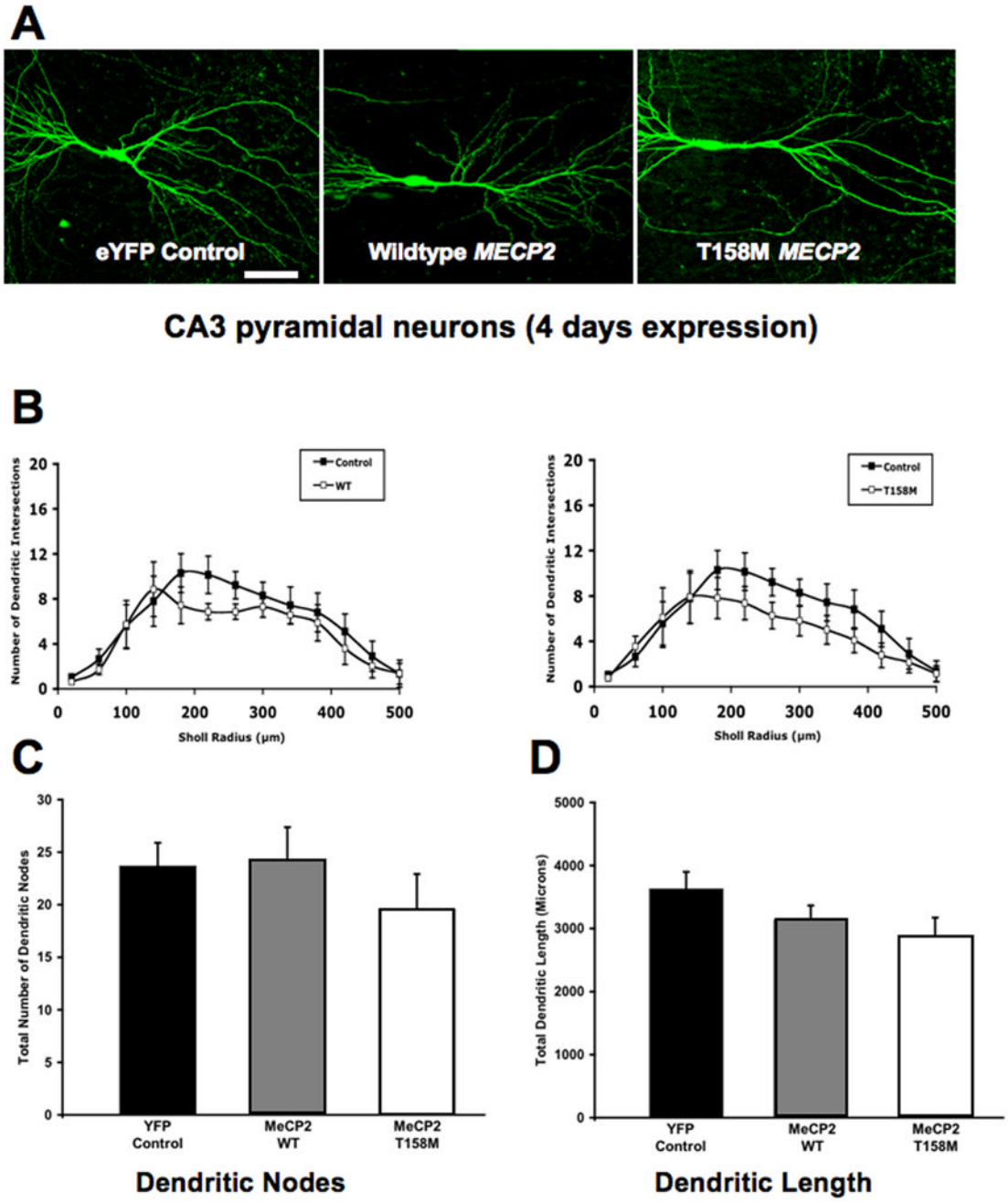

FIGURE 6. OVEREXPRESSION OF WILDTYPE *MECP2* TRANSIENTLY REDUCES THE NUMBER OF DENDRITIC NODES AND THE TOTAL DENDRITIC LENGTH, WHILE T158M *MECP2* TRANSIENTLY INCREASES DENDRITIC COMPLEXITY (4 DAYS OF EXPRESSION)

A. Representative low magnification views of eYFP-expressing CA3 pyramidal neurons transfected with either wildtype *MECP2* or the T158M *MECP2* mutant (4 days of expression). **B.** Three-dimensional Sholl analysis of dendritic complexity. Total number of intersections of CA3 apical dendrites as a function of distance from the soma. **C.** Total number of apical dendritic nodes. **D.** Total dendritic length.

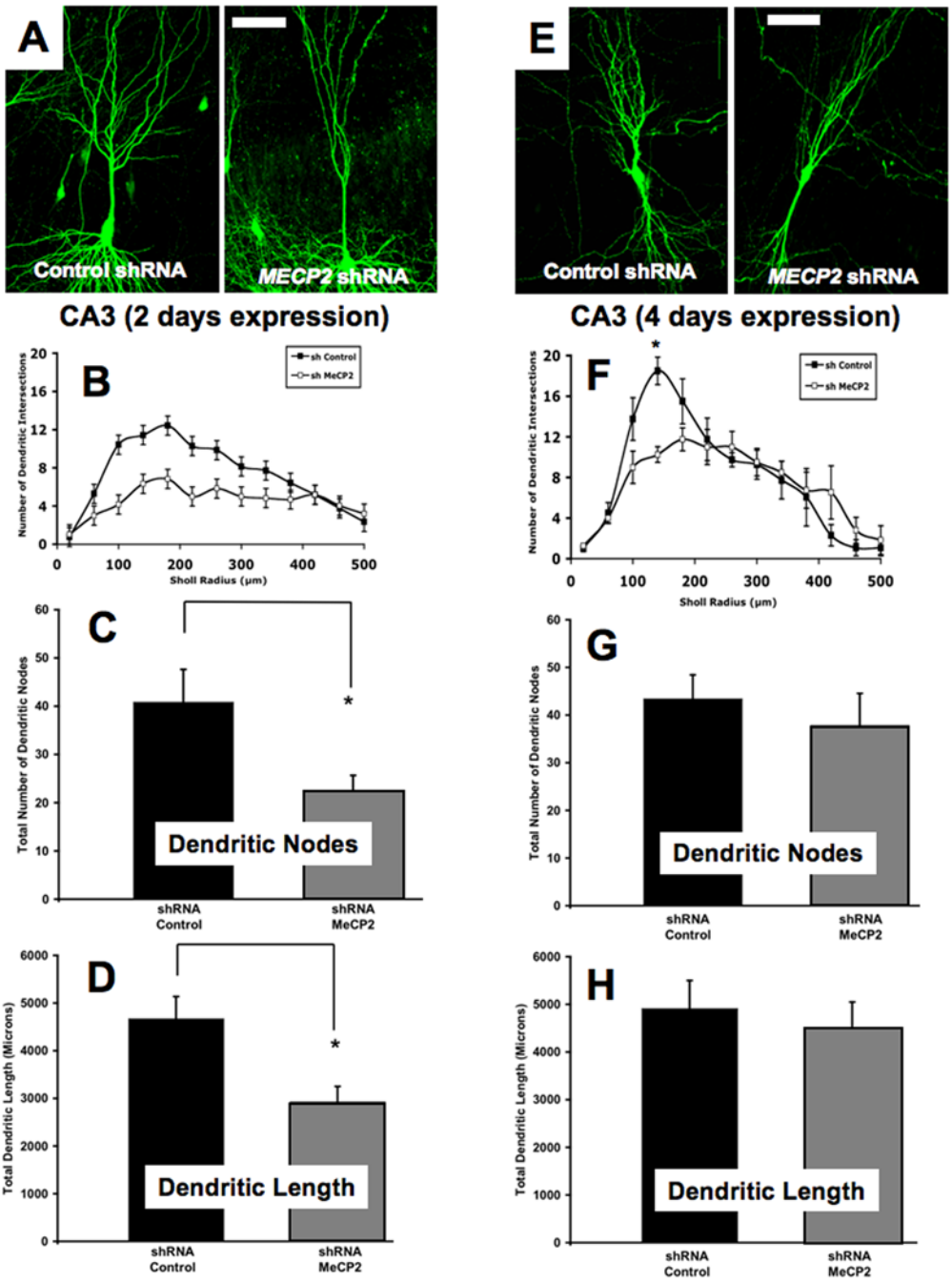

FIGURE 7. KNOCKDOWN OF ENDOGENOUS *MECP2* DECREASES THE NUMBER OF DENDRITIC NODES, TOTAL DENDRITIC LENGTH, AND DENDRITIC INTERSECTIONS

A. Representative low magnification views of eYFP-expressing CA3 pyramidal neurons transfected with an shRNA control plasmid or a specific shRNA interfering sequence designed to knockdown endogenous *Mecp2* (2 days of expression). **B.** Three-dimensional Sholl analysis of dendritic complexity. Total number of intersections of CA3 apical dendrites as a function of distance from the soma. **C.** Total number of apical dendritic nodes. **D.** Total dendritic length. **E.** Representative low magnification views of eYFP-expressing CA3 pyramidal neurons transfected with the shRNA control plasmid or the specific *Mecp2* shRNA (4 days of expression). **F.** Three-dimensional Sholl analysis of dendritic complexity. Total number of

intersections of CA3 apical dendrites as a function of distance from the soma. **G.** Total number of apical dendritic nodes. **H.** Total dendritic length.

Table 1

AVAILABLE INFORMATION OF THE HUMAN BRAIN SAMPLES FOR THE ANALYSES OF DENDRITIC SPINE DENSITY FROM HIPPOCAMPAL PYRAMIDAL NEURONS

Individual code	Brain bank	Gender	Age in years	Cause of death	Average spine density (spines/10μm)	Total dendritic length (μm)
1284 (non-MR)	UMB	F	3	Drowning	12.26	1602.87
1377 (non-MR)	UMB	F	5	Drowning	7.82	641.75
4638 (non-MR)	UMB	F	15	MVA	10.10	777.54
1571 (non-MR)	UMB	F	18	MVA	10.14	1447.34
1101 (non-MR)	UMB	F	19	MVA	5.30	521.08
4786 (non-MR)	UMB	F	22	MVA	8.18	704.34
1792 (non-MR)	UMB	F	25	MVA	8.45	322.41
1380 (non-MR)	UMB	F	35	MVA	10.40	400.76
4643 (non-MR)	UMB	F	42	HASCVD	9.88	1338.74
6150 (Rett)	HBB	F	3	Cardiac Arrest	4.40	610.32
1194 (Rett)	UMB	F	5	Asphyxia	5.04	906.83
6100 (Rett)	HBB	F	10	Unknown	8.85	926.59
6176 (Rett)	HBB	F	15	MI	5.83	636.55
6355 (Rett)	HBB	F	16	Respiratory Failure	5.77	687.61
1420 (Rett)	UMB	F	21	Unknown	7.50	1854.55
1748 (Rett)	UMB	F	22	Unknown	9.99	2163.51
5741 (Rett)	HBB	F	25	Pneumonia	3.77	1073.66
5478 (Rett)	HBB	F	42	Unknown	3.73	416.80
5763 (Rett)	HBB	F	42	Pneumonia	5.87	355.07

Formalin-fixed human brain samples were obtained from either the University of Maryland (UMB) or Harvard Brain Bank (HBB). The Table lists all the information provided by the brain banks (ages in years, causes of death, and confidential non-identifier codes). Information about specific *MECP2* mutations in Rett syndrome samples was not available from the brain banks. The average spine density and total dendritic length for each individual is presented to provide a sense of the statistical sample analyzed.

For individual 4638 (non-MR), the cause of death resulted from chest injuries sustained in a motor vehicle accident (MVA). For individuals 1571 (non-MR), 1101 (non-MR), 4786 (non-MR), 1792 (non-MR), and 1380 (non-MR) the causes of death resulted from multiple injuries sustained in a MVA. For individual 4643 (non-MR), the cause of death resulted from complications of hypertension arteriosclerotic cardiovascular disease (HASCVD).

Individual 1194 (Rett) had a seizure disorder that was noted on the tissue information sheet. For individual 6176 (Rett), the cause of death resulted from a myocardial infarction (MI). For individuals 1420 (Rett) and 1748 (Rett), the cause of death resulted from complications of the disorder, however the specific complication was not provided on the tissue information sheet.

Table 2

TOTAL DENDRITIC LENGTH, PYRAMIDAL NEURONS AND HIPPOCAMPAL SLICES SAMPLED FOR QUANTITATIVE ANALYSES

Treatment	Treatment Duration	Total length of dendrites (μm)	Number of neurons	Number of slices
eYFP control	48hrs	4571.98	25	15
eYFP control	96hrs	4318.46	31	23
Wildtype *MECP2*	48hrs	3870.79	18	16
Wildtype *MECP2*	96hrs	4454.44	23	10
R106W *MECP2*	48hrs	1867.94	11	10
R106W *MECP2*	96hrs	4555.15	16	11
T158M *MECP2*	48hrs	5042.62	25	22
T158M *MECP2*	96hrs	6813.60	30	14
shRNA Control	48hrs	1514.67	12	10
shRNA Control	96hrs	2402.05	21	11
MECP2 shRNA	48hrs	1668.45	13	10
MECP2 shRNA	96hrs	1952.64	14	12

Total number of different CA1 and CA3 pyramidal neurons and hippocampal slices used for quantitative analyses of dendritic spine density and geometrical morphology. The total length of dendrites measured is presented to provide a sense of the statistical sample analyzed.